Title Page (European Journal of Neuroscience https://onlinelibrary.wiley.com/journal/14609568)

Title

Neuron- and microglial specific immunoexpression in steroid-independent male sexual behaviour in castrated B6D2F1 male mice

Authors

CHIANG, Vic Shao-Chih[1]; LIPKIN, Sophie [1]; MCCUSKER, Catherine D[2]; PARK, Jin Ho[1]

Affiliation

[1] Developmental and Brain Sciences, Department of Psychology, University of Massachusetts, Boston, MA, United States

[2] Department of Biology, University of Massachusetts, Boston, MA, United States

Running title (40 characters maximum)

Steroid-independent sexual behaviour

Corresponding author

CHIANG, Vic Shao-Chih

Address

Developmental and Brain Sciences, Department of Psychology, University of Massachusetts, Boston, MA, United States

E-mail address

V.chiang001@umb.edu

Conflict of interest

The authors declare no conflict of interests.

Total manuscript word count

8051 (including figure legends, excluding references)

Page count (excluding references): 29

Number of figures: 5, and 2 supplementary figures

Number of tables: 0

Abstract (maximum 250 words)

Sexual behaviour is the *sine qua non* for procreation for several species and is traditionally viewed to be regulated by sex steroid hormones. However, several species exhibit steroid-independent sexual behaviour, and its molecular understanding is only beginning to be uncovered. We do not yet have a cell-specific understanding of the roles non-neuronal cells play in this phenomenon. Forty B6D2F1 hybrid male mice underwent orchidectomy and some of them exhibited consistent ejaculatory reflexes at least 62 weeks post-orchidectomy over 11 sexual behaviour tests (>180 minutes each), defined as steroid-independent (SI) maters (21.80%), and those that do not, defined as SI non-maters (25%). Using flow cytometry, we compared the preoptic area immunoexpression in NeuN+ neurons and Iba1+ microglia between SI maters and SI non-maters (n = 6 per group). We found neuronal immunoexpression up-regulated for amyloid precursor protein and androgen receptor, as well as down-regulated for glucocorticoid receptor. In conjunction, microglial immunoexpression of amyloid precursor protein up-regulated. These data suggest there are cell-specific immunoexpression changes including a role of non-neuronal cells in steroid-independent male sexual behaviour.

Keywords (maximum 6): Steroid independent; sexual behaviour; B6D2F1hybrid male mice; mechanism; microglia

Graphic abstract (maximum 70 words)

Introduction

Behaviour integrates multimodal sensory data from the complex and changing environment, that feeds to the highly dynamic emotions, cognition, learning and memory that results in flexible and precise muscle contractions for manoeuvres of the elemental basis of behaviour, called behavioural motifs, that are part of longer-term goals for understanding motivation, instincts, needs and survival of the organism (reviewed in (Gomez-Marin *et al.*, 2014); reviewed in (Anderson & Perona, 2014)). A fundamental behaviour *sine qua non* for procreation and species survival for several species is sexual behaviour. Sexual behaviour can even be for cooperation (reviewed in (Garcia *et al.*, 2021)), dominance (reviewed in (Steinberg, 2020)), and bartering (reviewed in (Addessi & Bourgeois-Gironde, 2020)), not limited to the opposite sex (reviewed in (Monk *et al.*, 2019)) and conspecifics ((Pelé *et al.*, 2017)). The canonical view of the physiological regulations on sexual behaviour involves sex steroid hormones (reviewed in (Wei *et al.*, 2021)), but several lines of evidence in various species indicate the possibilities of steroid-independent sexual behaviour (reviewed in (Chiang & Park, 2020)).

One species that demonstrates steroid-independent sexual behaviour is the B6D2F1 male mouse, which is a hybrid of C57BL/6J females and DBA/2J males, as they have been shown repeatedly since the 1960s that ~30% of them exhibit male sexual behaviour months after orchidectomy (McGill & Tucker, 1964; Manning & Thompson, 1976; Clemens *et al.*, 1988). In addition to the intrinsic value of understanding the abstruse nature and challenging definition of sexual behaviour itself (reviewed in (Monk *et al.*, 2019)), comprehending steroid-independent sexual behaviour tender pivotal implications in a plethora of domains. These encompass, but not limited to, learning and memory observed from the consistency of this behaviour (Quintana *et al.*, 2018; Quintana, Birrel, *et al.*, 2019; Quintana, Gonzalez, *et al.*, 2019), ethics in terms of animal welfare (Korsgaard, 2018; Palmer *et al.*, 2018; Smith, 2020), and evolution vis-à-vis natural selection (Rooker & Gavrilets, 2020). On top of these, insights could also be attained for how environment and lifestyle shapes sexual behaviour (Habr *et al.*, 2009; Felício *et al.*, 2012; Macrini *et al.*, 2016; Violante-Soria *et al.*, 2019), individuality with regards to behaviour variations (reviewed in (Kempermann, 2019)), and sexual diversity (reviewed in (Diamond, 2021)).

Very little is known regarding molecular understanding of steroid-independent sexual behaviour, and we do not understand the cell-specificity and the roles of non-neuronal cells in its molecular mechanisms. In particular, astrocytes are now recognized to regulate behaviour (reviewed in (Nagai *et al.*, 2021)), and microglia has been implicated in forgetting (Wang *et al.*, 2020), cognitive impairment (Pinto *et al.*, 2020), and sociability (Xu *et al.*, 2020), and developmentally linked for sexual behaviour ((Lenz *et al.*, 2013). Several molecular mechanisms may be at play for steroid-independent sexual behaviour. For instance, the sex steroid receptors, androgen receptor (AR) and oestrogen receptor alpha (ERa) are the cognate receptors of sex steroid hormones, which are paramount for canonical sexual behaviour, may be activated through alternative ligands (reviewed in (Chiang & Park, 2020)). In addition to the sex steroid hormone receptors, there are other steroid hormone receptors, encompassing nuclear receptor subfamily 3, several GPCRs and ion channels, which interacts with each other in certain contexts (reviewed in (Spaanderman *et al.*, 2018)). All six nuclear steroid receptors including glucocorticoid receptor (GR), ERa and AR share substantial homology due to their origin from one common ancestral receptor (reviewed in (Spaanderman *et al.*, 2018)). Based on empirical data of related molecules, researchers speculate GR regulated sexual behaviour in the context of stress (reviewed in (Ralph *et al.*, 2016)). In tandem with these, a previous microarray study found down-regulated glucocorticoid-induced transcript 1 expression in in the medial preoptic area and the bed nucleus of the stria terminalis of SI mater compared to SI non-maters (Park *et al.*, 2010). This study also found increased amyloid precursor protein (*App)* gene expression from microarray, increased APP immunoexpression from western blot and relatively more causal evidence of APP role in steroid-independent MSB (Park *et al.*, 2010). Despite this microarray study did not find changes in AR, GR, and ERa at the global level, it is possible that cell type-specific changes may still be present.

Here, using the B6D2F1 hybrid male mice, we replicated findings from previous studies that a significant proportion exhibited ejaculatory reflexes months after orchidectomy (Park *et al.*, 2009; Templin *et al.*, 2019). Within our cohort, we replicated the two distinct sexual phenotypes, comprising of those illustrating consistent male sexual behaviour (MSB) across 62 weeks post-orchidectomy over 11 tests (steroid-independent SI maters), and those that never illustrated any MSB post-orchidectomy

(SI non-maters). We set out to test neuron and microglia-specific immunoexpression using flow cytometry of four candidate molecules, informed *a priori* from the literature, in the preoptic area (POA), an integral site for MSB (reviewed in (Tsuneoka & Funato, 2021)). We hypothesized there would be neuron and microglia-specific increase in APP immunoexpression, no change in AR and ERa immunoexpression, as well as neuron and microglia-specific decrease in GR immunoexpression, in SI maters compared to SI non-maters. This would imply molecular mechanisms involving APP and GR, for instance, through BDNF (reviewed in (MacPherson, 2017)), and dopamine 1 receptor ((Wu *et al.*, 2016), respectively, could be justified for data-driven hypothesis of further detailed dissection to comprehend steroid-independent sexual behaviour. This could subsequently result in cell-specific genetic manipulation of the behaviour through vanguard technology such as with the CRISPR-Cas system (Goell & Hilton, 2021), and chemomagnetics (Maeng *et al.*, 2021).

Materials & Method

Animals

Details of our animal model have been provided previously (Bharadwaj *et al.*, 2013). In brief, male B6D2F1 hybrid mice (*Mus musculus;* n = 40, RRID:MGI:5651959*)* were produced by crossing C57BL/6J females (RRID:IMSR_JAX:000664) with DBA/2J males (RRID:IMSR_JAX:000671). All males were bred and raised in the animal facility at the University of Massachusetts, Boston, weaned at 21 – 28 days, single-sex group-housed until the beginning of experiments (between 50 and 80 d of age), and individually housed afterwards for the rest of the experiments. All mice were housed in the same room, with cages individually ventilated by negative airflow to prevent inter-cage transmission of olfactory cues (Keller *et al.*, 2006; McCarthy *et al.*, 2017). Animals were given food (Teklad Global Rodent Diet 2016, Harlan Laboratories Inc.) and water *ad libitum* and maintained on a 12:12 light: dark cycle, with lights off at 1200 h EST. All procedures were performed according to the University of Massachusetts, Boston, IACUC (#IACUC2020). All surgeries and sacrifices that were performed were conducted while the animals were anaesthetized with isoflurane, and all efforts were made to minimize suffering including the handling methods (Guerra *et al.*, 2021).

Details of our sexual experience procedure have also been provided previously (McInnis *et al.*, 2016). In brief, C57BL/6J females were used as stimulus females for sexual experience and MSB testing. Females were ovariectomized in adulthood after at least one parturition and injected subcutaneously with oestradiol benzoate (MilliporeSigma; 10µg in 0.1 mL sesame oil) 48 h before testing followed by subcutaneous progesterone administration (Millipore Sigma; 400µg in 0.05 mL sesame oil) 3-6h before testing. The females were group-housed in the same colony room as the experimental males. B6D2F1 hybrid males were provided with sexual experience on four separate occasions before orchidectomy by introducing the stimulus female into the home cage and left overnight.

Assessment of male sexual behaviour

Details of our male sexual behaviour assessments have been provided previously (Templin *et al.*, 2019). In brief, after B6D2F1 hybrid males were surgically castrated with orchidectomy, they were allowed to recover for at least one week before assessing for MSB. B6D2F1 hybrid males were tested for MSB with stimulus females 11 times over 62 weeks after orchidectomy. We tested over 62 weeks due to COVID19 where we had to suspend any lab work for an extended period. MSB was tested under dim red light at least one hour into the dark phase of a light/dark cycle. All males were habituated at least 30 min before the introduction of the stimulus female in a 17.8 × 25.4 × 17.8 cm clear Plexiglas testing cage containing the male's home cage bedding, which had not been changed for at least 48 hours. The test began with the introduction of a hormone-treated stimulus female and videotaped for more than 180 minutes. The videos were scored by an observer for the presence of ejaculatory reflexes. From 37 weeks post-castration, we introduced social exposure to each experimental male and each stimulus female prior to MSB tests (reasons discussed below). Details of the social exposure have been provided previously (Wersinger & Rissman, 2000). In brief, each experimental male and stimulus female received social exposure with a gonad-intact male and female mice for three consecutive days before MSB. During each exposure, each social stimulus was individually placed in the subject's home cage for two min. After 11 MSB tests, males were considered as steroid-independent (SI) maters if they demonstrated ejaculatory reflexes over 40% of all 11 tests, plus over 40% of the last five tests. Males were considered as SI-non-maters if they never demonstrated any ejaculatory reflexes over the 11 tests.

Cell isolation

Cells were isolated using the Adult Brian Dissociation kit (Miltenyi Biotec, cat # 130-107-677) following the manufacturer's instructions with several modifications, based on recommendations (Jaeger *et al.*, 2020) and from optimization. Given that only four mice could be tractably handled each day, samples were pseudorandomly allocated on each day to include a mix of SI maters and SI non-maters, and one extra B6D2F1 hybrid male mice to provide extra cells for flow cytometry technical controls. Due to the small volume of the target brain region (preoptic area), kidneys were used as carrier cells to improve cell retention during the dissociation, being an easily dissociable organ, and do

not substantially contaminate with cells expressing markers of nervous system cells common for other easily dissociable organs such as the prostate (Haga *et al.*, 2019) and the spleen (Pislyagin *et al.*, 2017). Mice (n = 16) were rapidly decapitated, then the brains and kidneys were rapidly extracted ensued by full immersion into ice-cold Dulbecco's PBS (Thermo Fisher Scientific, cat# 21600010; free of Mg^{2+} & Ca^{2+}; filter-sterilized with 0.22μm filter). The preoptic area (POA) was isolated using a brain matrix (Kent Scientific, cat # RBMA-200C) and surgical blades, immersed in ice-cold Dulbecco's PBS, under a dissection microscope. Alongside with kidney, the POA was finely minced in enzyme mix 1. After adding enzyme mix 2, the mixture was incubated in a hybridization chamber (Fisher Scientific, # 13-247-10) with maximum rotation (20min, 35°C). Ensuing that, the mixture was gently triturated with a 20G needle (Becton Dickinson, cat # 305175) and then further incubated (40min, 35°C). Enzymatic digestion was stopped by topping up to 15mL with DMEM (Gibco, cat# 12800017; added 3.7g/L sodium bicarbonate; adjusted to pH 7.2 – 7.4; filter-sterilized with 0.22μm filter) and added 0.1mg/mL ovomucoid protease inhibitor (Sigma, cat# T2011). The mixture was centrifuged (300 × *g*, 8min, 4°C) (Thermo Scientific, cat # 50136519) and then filtered through a 70 μm cell strainer (Fisher Scientific, cat # 352350) into a fresh 50mL conical tube, topped up to 20mL with DMEM. After centrifugation (300 × *g*, 8min, 4°C), we carried out the debris removal procedures according to the kit. The suspension was centrifuged with slow acceleration and deceleration rates (900 × *g*, 15 min, 4°C), then the supernatant was aspirated. Subsequent to that, the cell pellets were washed by topping up to 15mL with ice-cold Dulbecco's PBS and then centrifugation (300 × *g*, 10 min, 4°C) with full acceleration and brake. Following that, red blood cells were removed according to the kit with the incubation step under rotation with a mini rotator (speed 18, 4°C) (Fisher Scientific, cat # 88861052). To get a sense of the cell viability after these steps, cells were stained with trypan blue (Gibco, cat # 15250061), cover slipped onto a haemocytometer (Hausser Scientific, cat # 02-671-51B), and visualized under a fluorescent cell imager (Bio-Rad, cat # 1450031).

Staining

Cells were resuspended to a concentration of ~4 – 6 × 10^6 cells per ml and stained with 1µL of fixable viability dye, Zombie Aqua (Biolegend; cat# 423101), then incubated in the dark with rotation (room temperature, 30 minutes). The samples were washed with 1mL DMEM, centrifuged (300 × *g*, 8 min, room temperature) and aspirated until 100 µL remain. Subsequently, the cells were fixed using the Foxp3 / transcription factor staining buffer kit (eBioscience, cat # 00-5521-00) (according to the manufacturer's protocol with several modifications based on the recommendation (Reichard & Asosingh, 2019) and optimization. After fixation, the samples were centrifuged (600 × *g*, 5 min, room temperature), supernatant aspirated, and then resuspended into 1:1 glycerol (Millipore, cat # 4750-1L): Dulbecco's PBS (~1 – 2 × 10^6 cells per ml). The samples were stored at -20 ^{o}C in the dark until permeabilization within two weeks. Before permeabilization, the samples were diluted 10 fold into autoclaved distilled H_2O and centrifuged (600 × *g*, 5 min, room temperature) followed with permeabilization according to the manufacturer's instruction. The samples were then divided to include technical controls of unstained control, compensation controls, crystallizable fragment receptor blocking control, and fluorescence minus one controls, as well as two subsamples from each sample to accommodate two different antibody panels, with each sample and control resuspended into 100µL of permeabilization buffer. Samples and relevant controls were added with 2 µL of crystallizable fragment receptor blocker (Miltenyi Biotec, cat # 130-092-575) and incubated in the dark with rotation (12min, 4°C). The cells were then incubated with the intracellular primary antibody, rabbit anti-Ionized calcium-binding adaptor molecule 1 (Iba1; Fujifilm Wako; cat# 019-19741; RRID:AB_839504; polyclonal; 1:100; 0.5 mg/mL) in the dark with rotation (30min, room temperature). Following that, the cells were washed thrice with 1mL Dulbecco's DPBS and centrifugation (600 × *g*, 5 min, room temperature)(Eppendorf, cat # 5424R). Afterwards, the samples and relevant controls were incubated with the secondary antibody, Alexa Fluor 568-conjugated goat anti-rabbit IgG (H+L) (IgG-AF568; Invitrogen; cat# A-11011; RRID:AB_143157; polyclonal; 1:100; 2mg/mL) and the following directly conjugated antibodies: fluorescein isothiocyanate-conjugated rabbit anti-NeuN (NeuN-FITC; Abcam; cat# ab223994; RRID:AB_2892735; monoclonal EPR12763; 1:100; 0.5mg/mL); phycoerythrin-conjugated mouse anti-androgen receptor (AR-PE; R&D Systems; cat# IC5876P; RRID:AB_10890613;

monoclonal 523339; 1:10); allophycocyanin-conjugated mouse anti-oestrogen receptor alpha (Erα-APC; Novus Biologicals; cat# NB300-560; RRID:AB_10001032; monoclonal 33; 1:50; 1mg/mL); phycoerythrin-conjugated rabbit anti-amyloid precursor protein (APP-PE; Abcam; cat# ab208744; RRID:AB_2892736; monoclonal Y188; 1:1000; 0.5mg/mL); and allophycocyanin-conjugated mouse anti-glucocorticoid receptor (GR-APC; Invitrogen; cat# 17-6189-82; RRID:AB_2811764; monoclonal BuGR2; 1:200; 0.2mg/mL). These antibodies were selected based on the intended instrument, its spectral signatures, the antigen density to match fluorophore brightness, and available fluorophores for that antibody (Ferrer-Font *et al.*, 2020). In supplementary to these, on the basis of prevalent issues of antibody in terms of specificity, reproducibility and selectivity (Hsu *et al.*, 2020), we also selected antibodies from reputable vendors that validated the antibody and cited by existing studies. Anti-Iba1 was validated using mouse retinal whole-mount and cited in an erythro-myeloid progenitors study (Mass *et al.*, 2017). Anti-rabbit IgG-AF568 was validated using rat cerebellum and cited in a wind navigation study (Okubo *et al.*, 2020). Anti-NeuN-FITC was validated with flow cytometry using PC12 cells and cited in a viral encephalitis study (Michael *et al.*, 2020). Anti-AR-PE was validated with flow cytometry using LNCaP cells and cited in a cortical thymic epithelial cell study (Rode & Boehm, 2012). Anti-ERα-APC was validated using human breast tissue and cited in a follicular atresia study (Yao *et al.*, 2020). Anti-APP-PE was validated with flow cytometry using SH-SY5Y cells and cited in an adrenergic receptor study (Chena *et al.*, 2014). Anti-GR-APC was validated with flow cytometry using mouse splenocytes and cited in an endosomolytic peptide study (Akishiba *et al.*, 2017). After staining, samples were subjected to procedures in the Foxp3 / transcription factor staining buffer kit according to the manufacturer's protocol, then resuspended into Dulbecco's PBS for flow cytometry analysis.

Flow cytometry

The fluorescently stained populations (described above) were then analysed using a BD FACSAria Fusion with a 70 μm nozzle. Data was collected using BD FACSDiva software version 6.0 (http://www.bdbiosciences.com/instruments/software/facsdiva/index.jsp; RRID:SCR_001456). A compensation matrix was developed using singly stained and unstained controls of harvested cells.

Provisional gates were made using forward and side scatter of light to eliminate debris and non-singlet cells. Dead cells were then excluded using Zombie Aqua as well as Iba1 and NeuN as secondary markers to identify microglial and neuronal populations, respectively. AR, APP, GR and ERα expression were then analysed. Unstained and fluorescence minus one controls were used for correct placement of gates. As a benchmark for storage events, more than 30,000 NeuN+ neurons were acquired.

Flow cytometry bioinformatics

Data were analysed using FlowJo software version 10.6.1 (https://www.flowjo.com/solutions/flowjo; RRID:SCR_008520) following the recommended bioinformatics pipeline (Wang & Brinkman, 2019). The compensated data were quality assessed, and t transformed using the Logicle function. Subsequently, gating was carried out as described above using contour plots with outliers that show axis labels stating the marker and fluorochrome used, including numbers along the axes. A figure exemplifying the sequential flow cytometry gating strategy can be found in Supplementary Figure 1. Data on AR, APP, GR, and ERα were analysed from the contour plot showing the percentage of neurons or microglia, and from the histogram showing the distribution of the number of neurons or microglia at each fluorescence intensity. The percentage of cells of SI maters were normalized with a pseudorandomized pair with SI non-maters by division. Given flow cytometry data is log-normally distributed, and to be robust against outliers, the median fluorescent intensity (MdFI) was selected for the measure of expression (O'Neill *et al.*, 2013). The MdFI of SI maters were normalized with a pseudorandomized pair with SI non-maters by the resolution metric (Pinheiro *et al.*, 2020).

Statistical analyses

No statistical methods were used to predetermine sample sizes, but the sample size for flow cytometry experiments was determined empirically using standards generally employed by the field (Esk *et al.*, 2020; Farmen *et al.*, 2021; Sanmarco *et al.*, 2021), and sample size for sexual behaviour

testing were based on our previous studies (McInnis *et al.*, 2016). Biologically independent samples represent six SI maters, and six SI non-maters were used for flow cytometry. Given that there were more than six SI maters and non-maters in our mice cohort, we randomly selected six SI maters and six SI non-maters for flow cytometry. Experiments were performed blinded for annotating MSB videos to the history of ejaculatory reflexes of each mouse, during flow cytometry sample preparation, flow cytometry and bioinformatics analyses. All statistical analyses were performed using SPSS version 28 (https://www.ibm.com/products/spss-statistics; RRID:SCR_019096) and graphs made with GraphPad Prism version 9.0.0 (http://www.graphpad.com/; RRID:SCR_002798). Formal outlier tests were conducted using Grubb's test to determine outlying datapoints, then excluded from the analysis. The final sample size use for each analysis is shown in the figure legends. Most of the data fulfilled the assumption of Normality based on the Shapiro-Wilks test, without multivariate outliers based on the Mahalanobis distance, but do not fulfil the assumption of the homogeneity of variance based on Levene's test. Therefore, we proceeded with the non-parametric test, Mann-Whitney *U* test to compare between SI maters and SI non-maters with the threshold for significance set at $p < 0.05$. Statistical details for specific analysis, including exact *n* values and what *n* represents, statistical tests used, central tendency measure, *U* values, *P* values, effect sizes, and all plotted data points, can be found in the figure legends.

Results

B6D2F1 male mice exhibit male sexual behaviour 62 weeks after orchidectomy

At five weeks post-orchidectomy, 50% of the B6D2F1 exhibited ejaculatory reflex (Figure 1A). Following that, due to COVID19, we had to suspend any lab work for an extended period. Upon returning to the lab at 28 weeks post-orchidectomy, none of the B6D2F1 exhibited ejaculatory reflex (Figure 1A). We speculated this could be reasons for extended social isolation with the absence of physical exposure to other mice (Liu *et al.*, 2019), minimal human handling (Cho *et al.*, 2021), or ageing (Sokolov *et al.*, 2021). In accordance with our values in animal ethics to reduce the use of animals, to generate more outcomes, justified euthanasia, and reduce waste (reviewed in (Smith, 2020)), we attempted to salvage this experiment drew from these speculations. On the grounds of adversities to sexual behaviour with social isolation with extended periods of not physically interacting with other mice and the intertwined neurocircuit of sexual behaviour with other social behaviour (reviewed in Wei et al., 2021), we provided multiple social exposures prior to each sexual behaviour testing. The repeated sexual behaviour testing and social exposure correlated with an increase in the percentage of males exhibiting ejaculatory reflex back to levels quasi to previous studies with 28.13% at 43 weeks post-orchidectomy and 25% at 62 weeks post-orchidectomy (Figure 1A). Previous studies have unearthed two distinct sexual phenotypes in these post- orchiectomized B6D2F1 males, namely, the steroid-independent (SI) maters that consistently exhibit MSB and SI non-maters that do not (Park *et al.*, 2009; Bharadwaj *et al.*, 2013; Templin *et al.*, 2019). In general, these studies defined SI maters as those who demonstrated ejaculatory reflex on at least three out of the last four tests, including during the last test, and SI non-maters as those not demonstrating ejaculatory reflex on the last four tests (Park *et al.*, 2009; Bharadwaj *et al.*, 2013; Templin *et al.*, 2019). Given changes to our paradigm due to COVID19 with multiple confounders, we could not utilize the same definition. Instead, we defined SI maters as those that exhibited ejaculatory reflex at least 40% across all 11 tests, and at least 40% in the last 5 tests, and SI non-maters, that never exhibited ejaculatory reflex across all 11 tests. Our statistical analysis showed SI maters do *bona fide* exhibit increased ejaculatory reflex compared to non-maters

(Median ejaculatory reflex: SI maters = 7; SI non-maters = 0. Mann-Whitney U nonparametric statistical test, two-tailed, SI mater, *n* = 6 mice; SI non-mater, *n* = 6 mice, *p*-value = 0.002, U-value = 0.000, and effect size = 0.892) (Figure 1B). In summary, B6D2F1 male mice exhibited male sexual behaviour 62 weeks after orchidectomy including two distinct sexual phenotypes, SI maters and SI non-maters.

Steroid-independent maters exhibited altered amyloid precursor protein expression

We next investigated how SI MSB may be regulated at the molecular level using flow cytometry of the POA. Our first target was APP since a previous study found increased APP in SI maters compared to SI non-maters (Park *et al.*, 2010). Based on the APP MdFI from the flow cytometry histogram of the SI maters, which was normalized to the SI non-maters using the resolution metrics, we found a decrease in APP immunoexpression in POA neurons (Median MdFI resolution metrics: SI maters neuron = -0.0232; SI non-maters neuron = 0.000. Mann-Whitney U nonparametric statistical test, two-tailed, SI mater neuron, *n* = 5 mice; SI non-mater neuron, *n* = 6 mice, *p*-value = 0.003, *U*-value = 0.0000, and effect size = 0.9003) (Figure 2A, 2C). There were no changes to the percentage of neurons expressing APP from the flow cytometry contour plot of SI maters, which was normalized to the SI non-maters (Median normalized percentage of cells: SI maters neuron = 0.9113; SI non-maters neuron = 1.000. Mann-Whitney U nonparametric statistical test, two-tailed, SI mater neuron, *n* = 6 mice; SI non-mater neuron, *n* = 6 mice, *p*-value = 0.305, *U*-value = 12.000, and effect size = 0.2962.) (Figure 2B, 2D). This indicates that existing neurons expressing APP reduced APP immunoexpression.

There is a paucity of studies investigating non-neuronal cells in the brain in relation to sexual behaviour, therefore, we also investigated APP immunoexpression in Iba1+ microglia. We found an increase in APP expression in Iba1+ microglia of SI maters compared to non-maters (Median MdFI resolution metrics: SI maters microglia = 0.0124; SI non-maters microglia = 0.000. Mann-Whitney U nonparametric statistical test, two-tailed, SI mater microglia, n = 6 mice; SI non-mater microglia, n = 6 mice, p-value = 0.04, U-value = 6.000, and effect size = 0.5921) (Figure 2A, 2C). There were no

changes in the percentage of APP-expressing microglia in SI maters compared to non-maters (Median normalized percentage of cells: SI maters microglia = 0.9072; SI non-maters microglia = 0.000. Mann-Whitney U nonparametric statistical test, two-tailed, SI mater microglia, n = 6 mice; SI non-mater microglia, n = 6 mice, p-value = 1.000, U-value = 18.000, and effect size = 0.000). This indicates that existing microglia expressing APP increased APP immunoexpression.

Steroid-independent maters exhibit decreased androgen receptor expression in neurons

The sex steroid receptors, androgen receptor (AR) and oestrogen receptor alpha (ERa) are the cognate receptors of sex steroid hormones, which are paramount for canonical sexual behaviour (reviewed in (Chiang & Park, 2020)). Thus, we compared AR and ERa expression between SI maters and SI non-maters. We discovered a reduced AR expression in NeuN+ neuron of SI maters compared to SI non-maters (Median MdFI resolution metrics: SI maters neuron = -0.0115; SI non-maters neuron = 0.000. Mann-Whitney U nonparametric statistical test, two-tailed, SI mater neuron, n = 6 mice; SI non-mater neuron, n = 6 mice, p-value = 0.04, U-value = 6.0000, and effect size = 0.5921) (Figure 3A, C). In addition, we discovered a reduction in the percentage of AR-expressing neuron in SI maters compared to non-maters (Median normalized percentage of cells: SI maters neuron = 0.9602; SI non-maters neuron = 1.000. Mann-Whitney U nonparametric statistical test, two-tailed, SI mater neuron, n = 6 mice; SI non-mater neuron, n = 6 mice, p-value = 0.04, U-value = 6.000, and effect size = 0.5921) (Figure 3B, D). This indicates that there was an overall reduction of AR expression in SI mater neurons, and this could be related to the reduced neuronal population expressing AR. In terms of non-neuronal cells, Iba1+ microglia did not exhibit differential AR expression in SI maters compared to SI non-maters (Median MdFI resolution metrics: SI maters microglia = -0.007; SI non-maters microglia = 0.000. Mann-Whitney U nonparametric statistical test, two-tailed, SI mater microglia, *n* = 6 mice; SI non-mater microglia, *n* = 6 mice, *p*-value = 1.000, *U*-value = 18.000, and effect size = 0.000) (Figure 3A, C). In tandem with this, there were no changes in the percentage of Iba1+ neurons expressing AR in SI maters compared to SI non-maters (Median normalized percentage of cells: SI maters microglia = 0.9737; SI non-maters microglia = 0.000. Mann-Whitney U nonparametric statistical test, two-tailed, SI

mater microglia, *n* = 6 mice; SI non-mater microglia, *n* = 6 mice, *p*-value = 0.305, *U*-value = 12.000, and effect size = 0.2962) (Figure 3B, D). By the same token, we examined ERa, but there were no differences detected between SI maters and SI non-maters (Supplementary Figure 2).

Steroid-independent maters exhibit increased glucocorticoid receptor expression in neurons

Finally we investigated cell heterogeneous expression of GR on the grounds of its homology with ERa and AR (reviewed in (Spaanderman *et al.*, 2018), down-regulated glucocorticoid-induced transcript 1 expression in SI mater compared to SI non-maters (Park *et al.*, 2010), and GR regulation of sexual behaviour in the context of stress (reviewed in (Ralph *et al.*, 2016)). We unearthed an increased GR expression in NeuN+ neuron of SI maters compared to SI non-maters (Median MdFI resolution metrics: SI maters neuron = 0.0698; SI non-maters neuron = 0.000. Mann-Whitney U nonparametric statistical test, two-tailed, SI mater neuron, n = 6 mice; SI non-mater neuron, n = 6 mice, p-value = 0.002, U-value = 0.000, and effect size = 0.8883) (Figure 4A, C). At the same time, there were no changes in the percentage of GR-expressing neuron in SI maters compared to non-maters (Median normalized percentage of cells: SI maters neuron = 0.8824; SI non-maters neuron = 1.000. Mann-Whitney U nonparametric statistical test, two-tailed, SI mater neuron, n = 5 mice; SI non-mater neuron, n = 6 mice, p-value = 0.550, U-value = 12.000, and effect size = 0.18). What this means is the existing neurons acquire higher GR expression. Apropos to comparing SI maters to SI non-maters microglia in the POA, GR expression was unchanged in terms of expression level (Median MdFI resolution metrics: SI maters microglia = 0.0015; SI non-maters microglia = 0.000. Mann-Whitney U nonparametric statistical test, two-tailed, SI mater microglia, *n* = 6 mice; SI non-mater microglia, *n* = 6 mice, *p*-value = 0.305, *U*-value = 12.000, and effect size = 0.2962), and percentage of GR-expressing microglia (Median normalized percentage of cells: SI maters microglia = 0.9441; SI non-maters microglia = 0.000. Mann-Whitney U nonparametric statistical test, two-tailed, SI mater microglia, *n* = 5 mice; SI non-mater microglia, *n* = 6 mice, *p*-value = 0.073, *U*-value = 6.000, and effect size = 0.54030).

Discussion

Sex steroid hormones are cardinal for sexual behaviour, however, people have observed sexual behaviour independent of sex steroid hormones in several species (reviewed in (Chiang & Park, 2020)). While we are beginning to understand the neuroscience of sexual behaviour (reviewed in (Lenschow & Lima, 2020)), how this occurs independently of sex steroid hormones remain enigmatic. Here, we showed for the first time a differential immunoexpression profile between SI maters and SI non-maters in a cell-specific manner. In terms of neurons, SI maters had down-regulated APP and AR immunoexpression in tandem with up-regulated GR immunoexpression. For microglia, SI maters demonstrated increased APP immunoexpression.

Our mice model illustrated MSB post-orchidectomy, but the ~25% in our final MSB test is slightly less than the one third observed in previous studies (reviewed in (Chiang & Park, 2020)). The discrepancy may lie in our extended testing due to COVID19 at 62 weeks post-orchidectomy and the social exposure introduced, however we still found sufficient populations of the two contrasting sexual phenotypes, SI maters and SI non-maters. Our sexual phenotypes were based on the ejaculatory reflex (Pattij *et al.*, 2005), thus grasping comprehensive sexual behaviour parameters could garner more meaningful phenotypic demarcations (reviewed in (Heijkoop *et al.*, 2018)). This endeavour could now leverage machine learning approaches to make this daunting task tractable (reviewed in (Ebbesen & Froemke, 2021); reviewed in (Mathis *et al.*, 2020); reviewed in (Datta *et al.*, 2019)).

The development of sexual behaviour begins perinatally and peripubertally from the organizational effects of sex steroid hormones, followed by activation effects during adulthood (reviewed in (Balthazart, 2020)). We are therefore captivated by conceivable development differences in our target molecules that resulted in deviating sexual phenotypes. For instance, we found a down-regulated neuronal AR immunoexpression in SI maters compared to SI non-maters, which is the cognate receptor for androgens. This result seemingly contrasts to the previous microarray study finding no differences in *Ar* expression between these groups (Park *et al.*, 2010), and chronic AR blockers deemed ineffective to abate SIMSB ((Park *et al.*, 2009). However, this may be explained

through our study of AR at the translational level, and that down-regulated AR may be capacitating SIMSB.

During development, complementary to neuronal roles to shape sexual behaviour, non-neuronal cells drive spinogenesis essential for sexual behaviour by augmenting the production of prostaglandin E2 (Lenz *et al.*, 2013, 2018). We did find up-regulated microglial APP in SI maters compared to SI non-maters, in concordance to the previous study of APP up-regulation (Park *et al.*, 2010). The neuronal results for APP ostensibly contradicts this previous study, but it could be that microglial APP up-regulation may compensate for any down-regulation of neuronal APP at the global level. The role of microglia during sexual behaviour in adulthood are unknown. It is plausible this phenomenon likewise to those during development, drive spinogenesis by virtues of abundant spinogenesis occurring during adult sexual behaviour, in part through oxytocinergic signalling (Melis *et al.*, 2007; Becker *et al.*, 2013, 2015, 2017).

The discrepancy of our GR result of neuronal up-regulation similarly contrasts to the microarray study (Park *et al.*, 2010). In addition to the above rationale, another explanation alludes to the extra variables present in our mice apropos to age, social exposure, and sexual experience (Zancan *et al.*, 2018) that in spite of different trajectories still resulted in the same phenotype i.e. all roads lead to Rome. This suggest there may be multiple mechanisms of SIMSB at play that constitutes of redundant and compensatory pathways.

From these findings, and supporting studies from the literature, we composed a putative signalling pathway for SIMSB (Figure 5). Our targets APP, AR, and GR interact with molecules related to sexual behaviour, namely BDNF (Brague et al., 2018; reviewed in MacPherson, 2017), ERK (reviewed in (Jean *et al.*, 2017), (Kirouac *et al.*, 2017)), CREB (Barrot *et al.*, 2005; Sun *et al.*, 2021), nitric oxide (reviewed in (Will *et al.*, 2014)(Melis, 1998; Gu *et al.*, 2020)), glutamate (reviewed in (Chiang & Park, 2020)(Numakawa *et al.*, 2009)), and dopamine 1 receptor (reviewed in (Will *et al.*, 2014)(Melis *et al.*, 2003; Wu *et al.*, 2016)). They also interact with each other such that AR binds to APP (Takayama *et al.*, 2019), AR increases GR transcription (Spaanderman *et al.*, 2018)and GR induce secretase processing of APP (Baglietto-Vargas *et al.*, 2013).

Several limitations should be addressed in our study that require future studies to elaborate on. First alluded to the prevalent issue with antibodies that mandate orthogonal and parallel methods including artificial manipulation of target expression, to verify their specificity (Hsu *et al.*, 2020). Second, our single-suspension protocol biased the survival of certain cells, because quasi to most other flow cytometry protocols, we did not add reagents to improve neuron survival. This is reflected in the percentages we obtained for AR- and GR-expressing neurons, that differ to the ~40% of posistively expressing cells in a single-cell RNA-sequencing study (Moffitt *et al.*, 2018). Third were the cell markers we used, where Iba1 could be contaminated with border-associated macrophages (reviewed in (Eme-Scolan & Dando, 2020) and NeuN may disappear in neurons in certain contexts (reviewed in (Gusel'nikova & Korzhevskiy, 2015)). Finally, our work would benefit from deep learning tools for automated gating that decrease subjectivity, and increase analytical efficiency with higher dimensional data (reviewed in (Cheung *et al.*, 2021)).

Our findings of molecular differences between SI mater and SI non-maters warrants future research questions in behaviomics, evolution, and sexual diversity. Which comprehensive and multimodal parameters in sexual behaviour i.e. behaviomics (von Ziegler *et al.*, 2021), may correlate with APP immunoexpression levels? How may GR engender evolutionary difference (Carroll *et al.*, 2011; Rooker & Gavrilets, 2020) of species exhibiting SIMSB, and those that do not? Given that differential sensitivity to sex steroid hormone during development correlated with homosexuality (reviewed in (Balthazart, 2020)), what role does AR play in sexual diversity independent of steroid hormones? How does sensorimotor transformation occur in SIMSB including during ejaculation (Oti *et al.*, 2016, 2018, 2021; Kozyrev & Coolen, 2017)?

In summary, we report for the first time cell-specific differential immunoexpression of AR, GR, and APP in contrasting sexual phenotypes, defined on whether or not they exhibited consistent ejaculatory reflexes over the long term after orchidectomy. Overall, this paves the way to disentangle the intricate systems relevant to these molecules, as well as the behaviomics, diversity, and evolutionary lens on this phenomenon.

Acknowledgements: We thank Kaylee Wells of the UMass Boston Flow Cytometry Core for support on the BD FACSAria Fusion. We thank Dr Caroline David for assistance with animal husbandry, Benny Wan for assistance with surgeries, and other Park Lab members for general assistance. We thank Renjie Stephen Hu for help with figures production.

Author contributions: JHP and VSCC conceived and designed the experiments. VSCC performed the experiments and data analysis with help from SL. CDM supervised the flow cytometry. VSCC created the figures and wrote the manuscript with input from JHP. JHP, CDM and VSCC reviewed and edited the manuscript. JHP supervised the study, provided the resources, and acquired the funding.

Conflict of interest statement: The authors declare no conflict of interests

Abbreviations: AF568, Alexa Fluor 568; APC, allophycocyanin; APP, amyloid precursor protein; AR, androgen receptor; ERa, oestrogen receptor alpha; FITC, fluorescein isothiocyanate; GR, glucocorticoid receptor; Iba1, Ionized calcium-binding adaptor molecule 1; MdFI, median fluorescent intensity; MSB, male sexual behaviour; PE, phycoerythrin; POA, preoptic area; SI, steroid-independent

Data availability

Any data and materials that can be shared will be released via a material transfer agreement. Full access to biological data will be granted to collaborating scientists who are willing to complete a “Data Access Agreement” and a “Data Access Application form” and in accordance with General Data Protection Regulation.

Additional Information

Supplementary Information: Supplementary material available at the end of this manuscript.

Correspondence and requests for materials: Should be addressed to VSC.

Peer review information: Thanks in advance to the editorial team and reviewers for their contribution to the peer review of this work.

Figure Legends

Figure 1. B6D2F1 male mice exhibited male sexual behaviour 62 weeks after orchidectomy.

A) Percentage of B6D2F1 male mice exhibited ejaculatory reflex 62 weeks after orchidectomy across 11 tests.

B) Quantification of the number of ejaculatory reflexes exhibited by B6D2F1 male mice across 62 weeks after orchidectomy across 11 tests between SI maters and SI non-maters. Data: box and whisker plot showing median with min-max values, data points represent individual samples. Median ejaculatory reflex: SI maters = 7; SI non-maters = 0. Mann-Whitney U nonparametric statistical test, two-tailed, SI mater, n = 6 mice; SI non-mater, n = 6 mice, p-value = 0.002, U-value = 0.000, and effect size = 0.892.

** $p<0.01$; SI, steroid-independent

Figure 2. Steroid-independent maters exhibited altered amyloid precursor protein expression in preoptic area microglia and neuron compared to steroid-independent non-maters.

A) Representative flow cytometry histogram depicting overlay staining of anti-APP-PE in SI maters (solid line), non-maters (dotted line), and fluorescence minus one control without anti-APP-PE (dashed line), gated on preoptic area microglia (left) or neuron (right).

B) Representative flow cytometry contour plot of percentage of APP-expressing microglia or neuron in the preoptic area of SI maters (top), SI non-maters (middle), and fluorescence minus one control without anti-APP-PE (bottom).

C) Quantification of the MdFI resolution metrics of APP in the preoptic area neuron and microglia between SI maters and SI non-maters. Data: box and whisker plots showing median with min-max values, data points represent individual samples. Median MdFI resolution metrics: SI maters neuron = -0.0232; SI non-maters neuron = 0.000. Mann-Whitney U nonparametric statistical test, two-tailed, SI mater neuron, n = 5 mice; SI non-mater neuron, n = 6 mice, p-value = 0.003, U-value = 0.0000, and effect size = 0.9003. Median MdFI resolution metrics: SI maters microglia = 0.0124; SI non-maters microglia = 0.000. Mann-Whitney U nonparametric

statistical test, two-tailed, SI mater microglia, *n* = 6 mice; SI non-mater microglia, *n* = 6 mice, *p*-value = 0.04, *U*-value = 6.000, and effect size = 0.5921.

D) Quantification of the normalized percentage of APP-expressing neuron and microglia in preoptic area between SI maters and SI non-maters. Data: box and whisker plots showing median with min-max values, data points represent individual samples. Median normalized percentage of cells: SI maters neuron = 0.9113; SI non-maters neuron = 1.000. Mann-Whitney U nonparametric statistical test, two-tailed, SI mater neuron, *n* = 6 mice; SI non-mater neuron, *n* = 6 mice, *p*-value = 0.305, *U*-value = 12.000, and effect size = 0.2962. Median normalized percentage of cells: SI maters microglia = 0.9072; SI non-maters microglia = 0.000. Mann-Whitney U nonparametric statistical test, two-tailed, SI mater microglia, *n* = 6 mice; SI non-mater microglia, *n* = 6 mice, *p*-value = 1.000, *U*-value = 18.000, and effect size = 0.000.

APP, amyloid precursor protein; PE, phycoerythrin; MdFI, median fluorescence intensity; ns, not significant; * p<0.05; ** p<0.01; SI, steroid-independent

Figure 3. Steroid-independent maters exhibited decreased androgen receptor expression in preoptic area neurons compared to steroid-independent non-maters.

A) Representative flow cytometry histogram depicting overlay staining of anti-AR-PE in SI maters (solid line), non-maters (dotted line), and fluorescence minus one control without anti-AR-PE (dashed line), gated on preoptic area microglia (left) or neuron (right).

B) Representative flow cytometry contour plot of percentage of AR-expressing microglia or neuron in the preoptic area of SI maters (top), SI non-maters (middle), and fluorescence minus one control without anti-AR-PE (bottom).

C) Quantification of the MdFI resolution metrics of AR in the preoptic area neuron and microglia between SI maters and SI non-maters. Data: box and whisker plots showing median with min-max values, data points represent individual samples. Median MdFI resolution metrics: SI maters neuron = -0.0115; SI non-maters neuron = 0.000. Mann-Whitney U nonparametric statistical test, two-tailed, SI mater neuron, *n* = 6 mice; SI non-mater neuron, *n* = 6 mice, *p*-

value = 0.04, *U*-value = 6.0000, and effect size = 0.5921. Median MdFI resolution metrics: SI maters microglia = -0.007; SI non-maters microglia = 0.000. Mann-Whitney U nonparametric statistical test, two-tailed, SI mater microglia, *n* = 6 mice; SI non-mater microglia, *n* = 6 mice, *p*-value = 1.000, *U*-value = 18.000, and effect size = 0.000.

D) Quantification of the normalized percentage of AR-expressing neuron and microglia in preoptic area between SI maters and SI non-maters. Data: box and whisker plots showing median with min-max values, data points represent individual samples. Median normalized percentage of cells: SI maters neuron = 0.9602; SI non-maters neuron = 1.000. Mann-Whitney U nonparametric statistical test, two-tailed, SI mater neuron, *n* = 6 mice; SI non-mater neuron, *n* = 6 mice, *p*-value = 0.04, *U*-value = 6.000, and effect size = 0.5921. Median normalized percentage of cells: SI maters microglia = 0.9737; SI non-maters microglia = 0.000. Mann-Whitney U nonparametric statistical test, two-tailed, SI mater microglia, *n* = 6 mice; SI non-mater microglia, *n* = 6 mice, *p*-value = 0.305, *U*-value = 12.000, and effect size = 0.2962.

AR, androgen receptor; PE, phycoerythrin; MdFI, median fluorescence intensity; ns, not significant; * $p<0.05$; SI, steroid-independent

Figure 4. Steroid-independent maters exhibited increased glucocorticoid receptor expression in preoptic area neurons compared to steroid-independent non-maters.

A) Representative flow cytometry histogram depicting overlay staining of anti-GR-APC in SI maters (solid line), non-maters (dotted line), and fluorescence minus one control without anti-GR-APC (dashed line), gated on preoptic area microglia (left) or neuron (right).

B) Representative flow cytometry contour plot of percentage of GR-expressing microglia or neuron in the preoptic area of SI maters (top), SI non-maters (middle), and fluorescence minus one control without anti-GR-APC (bottom).

C) Quantification of the MdFI resolution metrics of GR in the preoptic area neuron and microglia between SI maters and SI non-maters. Data: box and whisker plots showing median with min-max values, data points represent individual samples. Median MdFI resolution metrics: SI

maters neuron = 0.0698; SI non-maters neuron = 0.000. Mann-Whitney U nonparametric statistical test, two-tailed, SI mater neuron, *n* = 6 mice; SI non-mater neuron, *n* = 6 mice, *p*-value = 0.002, *U*-value = 0.000, and effect size = 0.8883. Median MdFI resolution metrics: SI maters microglia = 0.0015; SI non-maters microglia = 0.000. Mann-Whitney U nonparametric statistical test, two-tailed, SI mater microglia, *n* = 6 mice; SI non-mater microglia, *n* = 6 mice, *p*-value = 0.305, *U*-value = 12.000, and effect size = 0.2962.

D) Quantification of the normalized percentage of GR-expressing neuron and microglia in preoptic area between SI maters and SI non-maters. Data: box and whisker plots showing median with min-max values, data points represent individual samples. Median normalized percentage of cells: SI maters neuron = 0.8824; SI non-maters neuron = 1.000. Mann-Whitney U nonparametric statistical test, two-tailed, SI mater neuron, *n* = 5 mice; SI non-mater neuron, *n* = 6 mice, *p*-value = 0.550, *U*-value = 12.000, and effect size = 0.18. Median normalized percentage of cells: SI maters microglia = 0.9441; SI non-maters microglia = 0.000. Mann-Whitney U nonparametric statistical test, two-tailed, SI mater microglia, *n* = 5 mice; SI non-mater microglia, *n* = 6 mice, *p*-value = 0.073, *U*-value = 6.000, and effect size = 0.5403.

GR, glucocorticoid receptor; APC, allophycocyanin; MdFI, median fluorescence intensity; ns, not significant; ** p<0.01; SI, steroid-independent

Figure 5. Putative signalling pathway regulating steroid independent male sexual behaviour

Based on our results, and their molecular targets relevant to sexual behaviour, we constructed a putative signalling pathway that may regulate steroid-independent male sexual behaviour. We observed neuron down-regulation of APP that can occur through BDNF up-regulation of alpha-secretase, which process APP into smaller fragments (reviewed in (MacPherson, 2017)). Canonical BDNF signalling occurs through binding to TrkB (reviewed in (MacPherson, 2017)). APP increase p-ERK (reviewed in (Jean *et al*., 2017)). We observed neuron down-regulation of AR, which can directly bind to APP (Takayama *et al*., 2019). AR also increase p-CREB, which drives transcription (Sun *et al.*, 2021) and induce p- NOS to produce NO (Gu *et al.*, 2020). We observed neuron up-regulation of GR, which can be mediated

through AR up-regulation of GR transcription (Spaanderman *et al.*, 2018). GR can then induce secretase processing of APP, not limited to alpha-secretase but other secretases including beta and gamma (Baglietto-Vargas *et al.*, 2013). Given that secretase processing decrease APP level, the balance of down-regulated AR, and up-regulated GR may result in the reduced APP. GR can complex with TrkB to trigger glutamate release (Numakawa *et al.*, 2009). GR can also up-regulate D1R (Wu *et al.*, 2016).

BDNF, Brain-Derived Neurotrophic Factor; TrkB, Tropomyosin receptor kinase B; GR, glucocorticoid receptor; APP, amyloid precursor protein; D1R, dopamine 1 receptor; G, Guanine nucleotide-binding proteins; $G_s\alpha$, G_s alpha subunit; G_{olf}, olfactory G; NO, nitric oxide ; p-, phosphorylate; NOS, nitric oxide synthase; AR, androgen receptor; ERK, Extracellular signal-regulated kinase;

Supplementary Figure Legends

Supplementary Figure 1. Gating strategy for identifying neuron and microglial populations from flow cytometry data.

Representative plots for the gating strategy used to identify populations of live as well as single microglia and neurons by flow cytometry for analysis. Arrows indicate the pre-gated parent population and the subsequent child population. Forward and side scatter of light were used to eliminate debris, and double exclusion of non-singlet cells by first forward scatter and then side scatter height versus weight. Dead cells were then excluded using fixable Zombie Aqua dye followed by Iba1 and NeuN as secondary markers to identify microglial and neuronal populations, respectively. Candidate molecules expression were then assessed in the Iba1+ and NeuN+ positive population. Unstained and fluorescence minus one controls were used for correct placement of gates.

Iba1, Ionized calcium-binding adaptor molecule 1; NeuN, Hexaribonucleotide Binding Protein-3; FITC, Fluorescein isothiocyanate;

Supplementary Figure 2. Steroid-independent maters do not differentially express oestrogen receptor alpha in preoptic area neurons compared to steroid-independent non-maters.

A) Representative flow cytometry histogram depicting overlay staining of anti-ERa-APC in SI maters (solid line), non-maters (dotted line), and fluorescence minus one control without anti-ERa-APC (dashed line), gated on preoptic area microglia (left) or neuron (right).
B) Representative flow cytometry contour plot of percentage of ERa-expressing microglia or neuron in the preoptic area of SI maters (top), SI non-maters (middle), and fluorescence minus one control without anti- ERa-APC (bottom).
C) Quantification of the MdFI resolution metrics of ERa in the preoptic area neuron and microglia between SI maters and SI non-maters. Data: box and whisker plots showing median with min-max values, data points represent individual samples. Median MdFI resolution metrics: SI maters neuron = -0.0005; SI non-maters neuron = 0.000. Mann-Whitney U nonparametric statistical test, two-tailed, SI mater neuron, n = 6 mice; SI non-mater neuron, n = 6 mice, p-

value = 1.000, *U*-value = 18.0000, and effect size = 0.000. Median MdFI resolution metrics: SI maters microglia = -0.0005; SI non-maters microglia = 0.000. Mann-Whitney U nonparametric statistical test, two-tailed, SI mater microglia, *n* = 6 mice; SI non-mater microglia, *n* = 6 mice, *p*-value = 0.305, *U*-value = 12.000, and effect size = 0.2962.

D) Quantification of the normalized percentage of ERa-expressing neuron and microglia in preoptic area between SI maters and SI non-maters. Data: box and whisker plots showing median with min-max values, data points represent individual samples. Median normalized percentage of cells: SI maters neuron = 0.7014; SI non-maters neuron = 1.000. Mann-Whitney U nonparametric statistical test, two-tailed, SI mater neuron, *n* = 6 mice; SI non-mater neuron, *n* = 6 mice, *p*-value = 0.305, *U*-value = 12.000, and effect size = 0.2962. Median normalized percentage of cells: SI maters microglia = 0.8053; SI non-maters microglia = 0.000. Mann-Whitney U nonparametric statistical test, two-tailed, SI mater microglia, *n* = 6 mice; SI non-mater microglia, *n* = 6 mice, *p*-value = 0.305, *U*-value = 12.000, and effect size = 0.2962.

ERa, oestrogen receptor alpha; APC, allophycocyanin; MdFI, median fluorescence intensity; ns, not significant; SI, steroid-independent

References

Addessi, E. & Bourgeois-Gironde, S. (2020) Are the roots of human economic systems shared with non-human primates? *Neurosci. Biobehav. Rev.*,.

Akishiba, M., Takeuchi, T., Kawaguchi, Y., Sakamoto, K., Yu, H.H., Nakase, I., Takatani-Nakase, T., Madani, F., Gräslund, A., & Futaki, S. (2017) Cytosolic antibody delivery by lipid-sensitive endosomolytic peptide. *Nat. Chem.*, **9**, 751–761.

Anderson, D.J. & Perona, P. (2014) Toward a science of computational ethology. *Neuron*,.

Baglietto-Vargas, D., Medeiros, R., Martinez-Coria, H., Laferla, F.M., & Green, K.N. (2013) Mifepristone alters amyloid precursor protein processing to preclude amyloid beta and also reduces tau pathology. *Biol. Psychiatry*, **74**, 357–366.

Balthazart, J. (2020) Sexual partner preference in animals and humans. *Neurosci. Biobehav. Rev.*,.

Barrot, M., Wallace, D.L., Bolaños, C.A., Graham, D.L., Perrotti, L.I., Neve, R.L., Chambliss, H., Yin, J.C., & Nestler, E.J. (2005) Regulation of anxiety and initiation of sexual behavior by CREB in the nucleus accumbens. *Proc. Natl. Acad. Sci. U. S. A.*, **102**, 8357–8362.

Becker, R.O., Dall'Oglio, A., Rigatto, K., Giovenardi, M., & Rasia-Filho, A.A. (2015) Differently shaped spines increase in the posterodorsal medial amygdala of oxytocin knockout female mice. *Neurosci. Res.*, **101**, 53–56.

Becker, R.O., Lazzari, V.M., Menezes, I.C., Morris, M., Rigatto, K., Lucion, A.B., Rasia-Filho, A.A., & Giovenardi, M. (2013) Sexual behavior and dendritic spine density of posterodorsal medial amygdala neurons in oxytocin knockout female mice. *Behav. Brain Res.*, **256**, 95–100.

Becker, R.O., Rasia-Filho, A.A., & Giovenardi, M. (2017) Selective deletion of the oxytocin gene remodels the number and shape of dendritic spines in the medial amygdala of males with and without sexual experience. *Neurosci. Lett.*, **660**, 155–159.

Bharadwaj, P., McInnis, C., Madden, A.M.K., Bonthuis, P.J., Zup, S., Rissman, E.F., & Park, J.H.

(2013) Increased Dendritic Spine Density and Tau Expression Are Associated with Individual Differences in Steroidal Regulation of Male Sexual Behavior. *PLoS One*, **8**.

Brague, J.C., Lenchur, C.N., Hayden, J.M., Davidson, R.H., Corrigan, K., Santini, G.T., & Swann, J.M. (2018) BDNF infusion into the MPN mag is sufficient to restore copulatory behavior in the castrated Syrian hamster. *Horm. Behav.*, **102**, 69–75.

Carroll, S.M., Ortlund, E.A., & Thornton, J.W. (2011) Mechanisms for the evolution of a derived function in the ancestral glucocorticoid receptor. *PLoS Genet.*, **7**, 1002117.

Chena, Y., Penga, Y., Chea, P., Gannona, M., Liua, Y., Lib, L., Bu, G., Van Groena, T., Jiaod, K., & Wanga, Q. (2014) α2A adrenergic receptor promotes amyloidogenesis through disrupting APP-SorLA interaction. *Proc. Natl. Acad. Sci. U. S. A.*, **111**, 17296–17301.

Cheung, M., Campbell, J.J., Whitby, L., Thomas, R.J., Braybrook, J., & Petzing, J. (2021) Current trends in flow cytometry automated data analysis software. *Cytom. Part A*,.

Chiang, V.S.C. & Park, J.H. (2020) Glutamate in Male and Female Sexual Behavior: Receptors, Transporters, and Steroid Independence. *Front. Behav. Neurosci.*,.

Cho, C., Chan, C., & Martin, L.J. (2021) Can Male Mice Develop Preference Towards Gentle Stroking by an Experimenter? *Neuroscience*, **464**, 26–32.

Clemens, L.G., Wee, B.E.F., Weaver, D.R., Roy, E.J., Goldman, B.D., & Rakerd, B. (1988) Retention of masculine sexual behavior following castration in male B6D2F1 mice. *Physiol. Behav.*, **42**, 69–76.

Datta, S.R., Anderson, D.J., Branson, K., Perona, P., & Leifer, A. (2019) Computational Neuroethology: A Call to Action. *Neuron*,.

Diamond, L.M. (2021) The New Genetic Evidence on Same-Gender Sexuality: Implications for Sexual Fluidity and Multiple Forms of Sexual Diversity. *J. Sex Res.*,.

Ebbesen, C.L. & Froemke, R.C. (2021) Body language signals for rodent social communication. *Curr. Opin. Neurobiol.*,.

Eme-Scolan, E. & Dando, S.J. (2020) Tools and Approaches for Studying Microglia In vivo. *Front. Immunol.*,.

Esk, C., Lindenhofe, D., Haendeler, S., Wester, R.A., Pflug, F., Schroeder, B., Bagley, J.A., Elling, U., Zuber, J., Von Haeseler, A., & Knoblich, J.A. (2020) A human tissue screen identifies a regulator of ER secretion as a brain-size determinant. *Science (80-.).*, **370**, 935–941.

Farmen, K., Nissen, S.K., Stokholm, M.G., Iranzo, A., Østergaard, K., Serradell, M., Otto, M., Svendsen, K.B., Garrido, A., Vilas, D., Borghammer, P., Santamaria, J., Møller, A., Gaig, C., Brooks, D.J., Tolosa, E., Pavese, N., & Romero-Ramos, M. (2021) Monocyte markers correlate with immune and neuronal brain changes in REM sleep behavior disorder. *Proc. Natl. Acad. Sci. U. S. A.*, **118**.

Felício, L.F., Couto-Moraes, R., de Oliveira, C.A., & Bernardi, M.M. (2012) Post-partum testosterone administration partially reverses the effects of perinatal cadmium exposure on sexual behavior in rats. *Psychol. Neurosci.*, **5**, 221–229.

Ferrer-Font, L., Pellefigues, C., Mayer, J.U., Small, S.J., Jaimes, M.C., & Price, K.M. (2020) Panel Design and Optimization for High-Dimensional Immunophenotyping Assays Using Spectral Flow Cytometry. *Curr. Protoc. Cytom.*, **92**.

Garcia, C., Bouret, S., Druelle, F., & Prat, S. (2021) Balancing costs and benefits in primates: Ecological and palaeoanthropological views. *Philos. Trans. R. Soc. B Biol. Sci.*,.

Goell, J.H. & Hilton, I.B. (2021) CRISPR/Cas-Based Epigenome Editing: Advances, Applications, and Clinical Utility. *Trends Biotechnol.*,.

Gomez-Marin, A., Paton, J.J., Kampff, A.R., Costa, R.M., & Mainen, Z.F. (2014) Big behavioral data: Psychology, ethology and the foundations of neuroscience. *Nat. Neurosci.*,.

Gu, L., Lian, D., Zheng, Y., Zhou, W., Gu, J., & Liu, X. (2020) Echinacoside□induced nitric oxide production in endothelial cells: Roles of androgen receptor and the PI3K□Akt pathway. *Int. J. Mol. Med.*, **45**, 1195–1202.

Guerra, S., Chesworth, R., Weickert, C.S., & Karl, T. (2021) Effects of handling on the behavioural phenotype of the neuregulin 1 type III transgenic mouse model for schizophrenia. *Behav. Brain Res.*, **405**.

Gusel'nikova, V. V. & Korzhevskiy, D.E. (2015) NeuN as a neuronal nuclear antigen and neuron differentiation marker. *Acta Naturae*,.

Habr, S.F., Dias, R.G., Teodorov, E., & Bernardi, M.M. (2009) Sexual experience did not affect the long-term sexual behavior inhibition of male rats treated with fluoxetine. *Psychol. Neurosci.*, **2**, 67–73.

Haga, N., Akaihata, H., Hata, J., Hiraki, H., Honda, R., Tanji, R., Onagi, A., Koguchi, T., Hoshi, S., Ogawa, S., Kataoka, M., Sato, Y., Ishibashi, K., & Kojima, Y. (2019) The association between local arteriosclerosis of the prostatic arteries and chronic inflammation in human benign prostatic enlargement. *Prostate*, **79**, 574–582.

Heijkoop, R., Huijgens, P.T., & Snoeren, E.M.S. (2018) Assessment of sexual behavior in rats: The potentials and pitfalls. *Behav. Brain Res.*,.

Hsu, C.-N., Chang, C.-H., Poopradubsil, T., Lo, A., William, K.A., Lin, K.-W., Bandrowski, A., Ozyurt, I.B., Grethe, J.S., & Martone, M.E. (2020) Antibody Watch: Text Mining Antibody Specificity from the Literature. *PLOS Comput. Biol.*, **17**, e1008967.

Jaeger, B.N., Yángüez, E., Gesuita, L., Denoth-Lippuner, A., Kruse, M., Karayannis, T., & Jessberger, S. (2020) Miniaturization of Smart-seq2 for Single-Cell and Single-Nucleus RNA Sequencing. *STAR Protoc.*, **1**, 100081.

Jean, A., Trouillet, A.C., Andrianarivelo, N.A., Mhaouty-Kodja, S., & Hardin-Pouzet, H. (2017) Phospho-ERK and sex steroids in the mPOA: Involvement in male mouse sexual behaviour. *J. Endocrinol.*, **233**, 257–267.

Keller, M., Pierman, S., Douhard, Q., Baum, M.J., & Bakker, J. (2006) The vomeronasal organ is required for the expression of lordosis behaviour, but not sex discrimination in female mice. *Eur. J.*

Neurosci., **23**, 521–530.

Kempermann, G. (2019) Environmental enrichment, new neurons and the neurobiology of individuality. *Nat. Rev. Neurosci.*,.

Kirouac, L., Rajic, A.J., Cribbs, D.H., & Padmanabhan, J. (2017) Activation of Ras-ERK signaling and GSK-3 by amyloid precursor protein and amyloid beta facilitates neurodegeneration in Alzheimer's disease. *eNeuro*, **4**.

Korsgaard, C.M. (2018) The Claims of Animals and the Needs of Strangers: Two Cases of Imperfect Right.

Kozyrev, N. & Coolen, L.M. (2017) Activation of galanin and cholecystokinin receptors in the lumbosacral spinal cord is required for ejaculation in male rats. *Eur. J. Neurosci.*, **45**, 846–858.

Lenschow, C. & Lima, S.Q. (2020) In the mood for sex: neural circuits for reproduction. *Curr. Opin. Neurobiol.*,.

Lenz, K.M., Nugent, B.M., Haliyur, R., & McCarthy, M.M. (2013) Microglia are essential to masculinization of brain and behavior. *J. Neurosci.*, **33**, 2761–2772.

Lenz, K.M., Pickett, L.A., Wright, C.L., Davis, K.T., Joshi, A., & McCarthy, M.M. (2018) Mast cells in the developing brain determine adult sexual behavior. *J. Neurosci.*, **38**, 8044–8059.

Liu, Z.W., Yu, Y., Lu, C., Jiang, N., Wang, X.P., Xiao, S.Y., & Liu, X.M. (2019) Postweaning isolation rearing alters the adult social, sexual preference and mating behaviors of male CD-1 mice. *Front. Behav. Neurosci.*, **13**.

MacPherson, R.E.K. (2017) Filling the void: A role for exercise-induced BDNF and brain amyloid precursor protein processing. *Am. J. Physiol. - Regul. Integr. Comp. Physiol.*,.

Macrini, D.J., Bonamin, L. V., Teodorov, E., Kirsten, T.B., Coelho, C.P., Motta, P.D., Ramos, L., Dalboni, L.C., Bondan, E.F., & Bernardi, M.M. (2016) Overweight male juvenile rats exhibit decreases in sexual behavior and serum testosterone levels and an increase in tnf-α levels in adulthood. *Psychol. Neurosci.*, **9**, 188–197.

Maeng, L.Y., Rosenfeld, D., Simandl, G.J., Koehler, F., Alexander, W., Moon, J., Varnavides, G., Murillo, M.F., Reimer, A.E., Wald, A., Anikeeva, P., & Widge, A.S. (2021) Running Title□: Magnetothermal Peripheral Organ Stimulation Affiliations□: 1–22.

Manning, A. & Thompson, M.L. (1976) Postcastration retention of sexual behaviour in the male BDF1 mouse: The role of experience. *Anim. Behav.*, **24**, 523–533.

Mass, E., Jacome-Galarza, C.E., Blank, T., Lazarov, T., Durham, B.H., Ozkaya, N., Pastore, A., Schwabenland, M., Chung, Y.R., Rosenblum, M.K., Prinz, M., Abdel-Wahab, O., & Geissmann, F. (2017) A somatic mutation in erythro-myeloid progenitors causes neurodegenerative disease. *Nature*, **549**, 389–393.

Mathis, A., Schneider, S., Lauer, J., & Mathis, M.W. (2020) A Primer on Motion Capture with Deep Learning: Principles, Pitfalls, and Perspectives. *Neuron*,.

McCarthy, E.A., Maqsudlu, A., Bass, M., Georghiou, S., Cherry, J.A., & Baum, M.J. (2017) DREADD-induced silencing of the medial amygdala reduces the preference for male pheromones and the expression of lordosis in estrous female mice. *Eur. J. Neurosci.*, **46**, 2035–2046.

McGill, T.E. & Tucker, G.R. (1964) Genotype and sex drive in intact and in castrated male mice. *Science (80-.).*, **145**, 514–515.

McInnis, C.M., Venu, S., & Park, J.H. (2016) Steroid-independent male sexual behavior in B6D2F2 male mice. *Horm. Behav.*, **85**, 26–29.

Melis, M.R. (1998) Nitric oxide production is increased in the paraventricular nucleus of the hypothalamus of male rats during non-contact penile erections and copulation. *Eur. J. Neurosci.*, **10**, 1968–1974.

Melis, M.R., Melis, T., Cocco, C., Succu, S., Sanna, F., Pillolla, G., Boi, A., Ferri, G.L., & Argiolas, A. (2007) Oxytocin injected into the ventral tegmental area induces penile erection and increases extracellular dopamine in the nucleus accumbens and paraventricular nucleus of the hypothalamus of male rats. *Eur. J. Neurosci.*, **26**, 1026–1035.

Melis, M.R., Succu, S., Mascia, M.S., Cortis, L., & Argiolas, A. (2003) Extra-cellular dopamine increases in the paraventricular nucleus of male rats during sexual activity. *Eur. J. Neurosci.*, **17**, 1266–1272.

Michael, B.D., Bricio-Moreno, L., Sorensen, E.W., Miyabe, Y., Lian, J., Solomon, T., Kurt-Jones, E.A., & Luster, A.D. (2020) Astrocyte- and Neuron-Derived CXCL1 Drives Neutrophil Transmigration and Blood-Brain Barrier Permeability in Viral Encephalitis. *Cell Rep.*, **32**.

Moffitt, J.R., Bambah-Mukku, D., Eichhorn, S.W., Vaughn, E., Shekhar, K., Perez, J.D., Rubinstein, N.D., Hao, J., Regev, A., Dulac, C., & Zhuang, X. (2018) Molecular, spatial, and functional single-cell profiling of the hypothalamic preoptic region. *Science (80-.).*, **362**.

Monk, J.D., Giglio, E., Kamath, A., Lambert, M.R., & McDonough, C.E. (2019) An alternative hypothesis for the evolution of same-sex sexual behaviour in animals. *Nat. Ecol. Evol.*,.

Nagai, J., Yu, X., Papouin, T., Cheong, E., Freeman, M.R., Monk, K.R., Hastings, M.H., Haydon, P.G., Rowitch, D., Shaham, S., & Khakh, B.S. (2021) Behaviorally consequential astrocytic regulation of neural circuits. *Neuron*,.

Numakawa, T., Kumamaru, E., Adachi, N., Yagasaki, Y., Izumi, A., & Kunugi, H. (2009) Glucocorticoid receptor interaction with TrkB promotes BDNF-triggered PLC-γ signaling for glutamate release via a glutamate transporter. *Proc. Natl. Acad. Sci. U. S. A.*, **106**, 647–652.

O'Neill, K., Aghaeepour, N., Špidlen, J., & Brinkman, R. (2013) Flow Cytometry Bioinformatics. *PLoS Comput. Biol.*, **9**.

Okubo, T.S., Patella, P., D'Alessandro, I., & Wilson, R.I. (2020) A Neural Network for Wind-Guided Compass Navigation. *Neuron*, **107**, 924-940.e18.

Oti, T., Sakamoto, T., & Sakamoto, H. (2021) Systemic effects of oxytocin on male sexual activity via the spinal ejaculation generator in rats. *Commun. Integr. Biol.*, **14**, 55–60.

Oti, T., Takanami, K., Ito, S., Ueda, T., Matsuda, K.I., Kawata, M., Soh, J., Ukimura, O., Sakamoto, T., & Sakamoto, H. (2018) Effects of sex steroids on the spinal gastrin-releasing peptide system

controlling male sexual function in rats. *Endocrinology*, **159**, 1886–1896.

Oti, T., Takanami, K., Katayama, N., Edey, T., Satoh, K., Sakamoto, T., & Sakamoto, H. (2016) Perinatal testosterone exposure is critical for the development of the male-specific sexually dimorphic gastrin-releasing peptide system in the lumbosacral spinal cord that mediates erection and ejaculation. *Biol. Sex Differ.*, **7**.

Palmer, C., Pedersen, H.G., & Sandøe, P. (2018) Beyond Castration and Culling: Should We Use Non-surgical, Pharmacological Methods to Control the Sexual Behavior and Reproduction of Animals? *J. Agric. Environ. Ethics*, **31**, 197–218.

Park, J.H., Bonthius, P.J., Tsai, H.W., Bekiranov, S., & Rissman, E.F. (2010) Amyloid β precursor protein regulates male sexual behavior. *J. Neurosci.*, **30**, 9967–9972.

Park, J.H., Bonthuis, P., Ding, A., Rais, S., & Rissman, E.F. (2009) Androgen- and estrogen-independent regulation of copulatory behavior following castration in male B6D2F1 mice. *Horm. Behav.*, **56**, 254–263.

Pattij, T., de Jong, T.R., Uitterdijk, A., Waldinger, M.D., Veening, J.G., Cools, A.R., van der Graaf, P.H., & Olivier, B. (2005) Individual differences in male rat ejaculatory behaviour: searching for models to study ejaculation disorders. *Eur. J. Neurosci.*, **22**, 724–734.

Pelé, M., Bonnefoy, A., Shimada, M., & Sueur, C. (2017) Interspecies sexual behaviour between a male Japanese macaque and female sika deer. *Primates*, **58**, 1–4.

Pinheiro, D.F., Szenes-Nagy, A.B., Maurano, M.M., Lietzenmayer, M., Klicznik, M.M., Holly, R., Kirchmeier, D., Kitzmueller, S., Achatz-Straussberger, G., Rosenblum, M.D., Thalhamer, J., Abbas, A.K., & Gratz, I.K. (2020) Cutting Edge: Tissue Antigen Expression Levels Fine-Tune T Cell Differentiation Decisions In Vivo. *J. Immunol.*, **205**, 2577–2582.

Pinto, B., Morelli, G., Rastogi, M., Savardi, A., Fumagalli, A., Petretto, A., Bartolucci, M., Varea, E., Catelani, T., Contestabile, A., Perlini, L.E., & Cancedda, L. (2020) Rescuing Over-activated Microglia Restores Cognitive Performance in Juvenile Animals of the Dp(16) Mouse Model of

Down Syndrome. *Neuron*, **108**, 887-904.e12.

Pislyagin, E.A., Manzhulo, I. V., Gorpenchenko, T.Y., Dmitrenok, P.S., Avilov, S.A., Silchenko, A.S., Wang, Y.M., & Aminin, D.L. (2017) Cucumarioside A2-2 causes macrophage activation in mouse spleen. *Mar. Drugs*, **15**.

Quintana, G.R., Birrel, M., Marceau, S., Kalantari, N., Bowden, J., Bachoura, Y., Borduas, E., Lemay, V., Payne, J.W., Cionnaith, C. Mac, & Pfaus, J.G. (2019) Differential disruption of conditioned ejaculatory preference in the male rat based on different sensory modalities by micro-infusions of naloxone to the medial preoptic area or ventral tegmental area. *Psychopharmacology (Berl).*, **236**, 3613–3623.

Quintana, G.R., Gonzalez, B., Borduas, E., Lemay, V., Yarur, F., & Pfaus, J.G. (2019) Naloxone Disrupts the Development of a Conditioned Ejaculatory Preference Based on a Somatosensory Cue in Male Rats. *Behav. Neurosci.*, **133**, 198–202.

Quintana, G.R., Jackson, M., Nasr, M., & Pfaus, J.G. (2018) Effect of CS preexposure on the conditioned ejaculatory preference of the male rat: Behavioral analyses and neural correlates. *Learn. Mem.*, **25**, 513–521.

Ralph, C.R., Lehman, M.N., Goodman, R.L., & Tilbrook, A.J. (2016) Impact of psychosocial stress on gonadotrophins and sexual behaviour in females: Role for cortisol? *Reproduction*,.

Reichard, A. & Asosingh, K. (2019) Best Practices for Preparing a Single Cell Suspension from Solid Tissues for Flow Cytometry. *Cytom. Part A*, **95**, 219–226.

Rode, I. & Boehm, T. (2012) Regenerative capacity of adult cortical thymic epithelial cells. *Proc. Natl. Acad. Sci. U. S. A.*, **109**, 3463–3468.

Rooker, K. & Gavrilets, S. (2020) On the evolution of sexual receptivity in female primates. *Sci. Rep.*, **10**, 11945.

Sanmarco, L.M., Wheeler, M.A., Gutiérrez-Vázquez, C., Polonio, C.M., Linnerbauer, M., Pinho-Ribeiro, F.A., Li, Z., Giovannoni, F., Batterman, K. V., Scalisi, G., Zandee, S.E.J., Heck, E.S.,

Alsuwailm, M., Rosene, D.L., Becher, B., Chiu, I.M., Prat, A., & Quintana, F.J. (2021) Gut-licensed IFNγ+ NK cells drive LAMP1+TRAIL+ anti-inflammatory astrocytes. *Nature*, **590**, 473–479.

Smith, A.J. (2020) Guidelines for planning and conducting high-quality research and testing on animals. *Lab. Anim. Res.*, **36**, 1–6.

Sokolov, O.Y., Prokhorova, T.A., Tereshkina, E.B., Zozulya, S.A., Simonov, A.N., Kost, N. V., Dadayan, A.K., Bogachouk, A.P., & Zolotarev, Y.A. (2021) Neurotropic peptide HLDF-6-amide reduces age-related decline in sexual activity in old male rats. *Exp. Gerontol.*, **149**.

Spaanderman, D.C.E., Nixon, M., Buurstede, J.C., Sips, H.H.C.M., Schilperoort, M., Kuipers, E.N., Backer, E.A., Kooijman, S., Rensen, P.C.N., Homer, N.Z.M., Walker, B.R., Meijer, O.C., & Kroon, J. (2018) Androgens modulate glucocorticoid receptor activity in adipose tissue and liver. *J. Endocrinol.*, **240**, 51–63.

Steinberg, D. (2020) Immoral-like Behavior in Animals. In *The Multidisciplinary Nature of Morality and Applied Ethics*. Springer International Publishing, pp. 37–44.

Sun, R.F., Zhao, C.Y., Chen, S., Yu, W., Zhou, M.M., & Gao, C.R. (2021) Androgen Receptor Stimulates Hexokinase 2 and Induces Glycolysis by PKA/CREB Signaling in Hepatocellular Carcinoma. *Dig. Dis. Sci.*, **66**, 802–813.

Takayama, K. ichi, Fujiwara, K., & Inoue, S. (2019) Amyloid precursor protein, an androgen-regulated gene, is targeted by RNA-binding protein PSF/SFPQ in neuronal cells. *Genes to Cells*, **24**, 719–730.

Templin, J.S., Wyrosdic, J.C., David, C.D., Wyrosdic, B.N., Lapp, H.E., Bala, A., Bartlett, A., Khan, Z., Rokicki, A., & Park, J.H. (2019) Peripubertal gonadal steroids are necessary for steroid-independent male sexual behavior in castrated B6D2F1 male mice. *Horm. Behav.*, **113**, 38–46.

Tsuneoka, Y. & Funato, H. (2021) Cellular Composition of the Preoptic Area Regulating Sleep, Parental, and Sexual Behavior. *Front. Neurosci.*,.

Violante-Soria, V., Cruz, S.L., & Rodríguez-Manzo, G. (2019) Sexual behaviour is impaired by the abused inhalant toluene in adolescent male rats. *Eur. J. Neurosci.*, **50**, 2113–2123.

von Ziegler, L., Sturman, O., & Bohacek, J. (2021) Big behavior: challenges and opportunities in a new era of deep behavior profiling. *Neuropsychopharmacology*,.

Wang, C., Yue, H., Hu, Z., Shen, Y., Ma, J., Li, J., Wang, X.D., Wang, L., Sun, B., Shi, P., Wang, L., & Gu, Y. (2020) Microglia mediate forgetting via complement-dependent synaptic elimination. *Science (80-.).*, **367**, 688–694.

Wang, S. & Brinkman, R.R. (2019) Data-driven flow cytometry analysis. In *Methods in Molecular Biology*. Humana Press Inc., pp. 245–265.

Wei, D., Talwar, V., & Lin, D. (2021) Neural circuits of social behaviors: Innate yet flexible. *Neuron*,.

Wersinger, S.R. & Rissman, E.F. (2000) Dopamine activates masculine sexual behavior independent of the estrogen receptor α. *J. Neurosci.*, **20**, 4248–4254.

Will, R.G., Hull, E.M., & Dominguez, J.M. (2014) Influences of dopamine and glutamate in the medial preoptic area on male sexual behavior. *Pharmacol. Biochem. Behav.*, **121**, 115–123.

Wu, B., Liang, Y., Dong, Z., Chen, Z., Zhang, G., Lin, W., Wang, S., Wang, B., Ge, R.S., & Lian, Q. (2016) Glucocorticoid receptor mediated the propofol self-administration by dopamine D1 receptor in nucleus accumbens. *Neuroscience*, **328**, 184–193.

Xu, Z.X., Kim, G.H., Tan, J.W., Riso, A.E., Sun, Y., Xu, E.Y., Liao, G.Y., Xu, H., Lee, S.H., Do, N.Y., Lee, C.H., Clipperton-Allen, A.E., Kwon, S., Page, D.T., Lee, K.J., & Xu, B. (2020) Elevated protein synthesis in microglia causes autism-like synaptic and behavioral aberrations. *Nat. Commun.*, **11**, 1–17.

Yao, J., Ma, Y., Zhou, S., Bao, T., Mi, Y., Zeng, W., Li, J., & Zhang, C. (2020) Metformin prevents follicular atresia in aging laying chickens through activation of PI3K/Akt and calcium signaling pathways. *Oxid. Med. Cell. Longev.*, **2020**.

Zancan, M., da Cunha, R.S.R., Schroeder, F., Xavier, L.L., & Rasia-Filho, A.A. (2018) Remodeling of

the number and structure of dendritic spines in the medial amygdala: From prepubertal sexual dimorphism to puberty and effect of sexual experience in male rats. *Eur. J. Neurosci.*, **48**, 1851–1865.

944

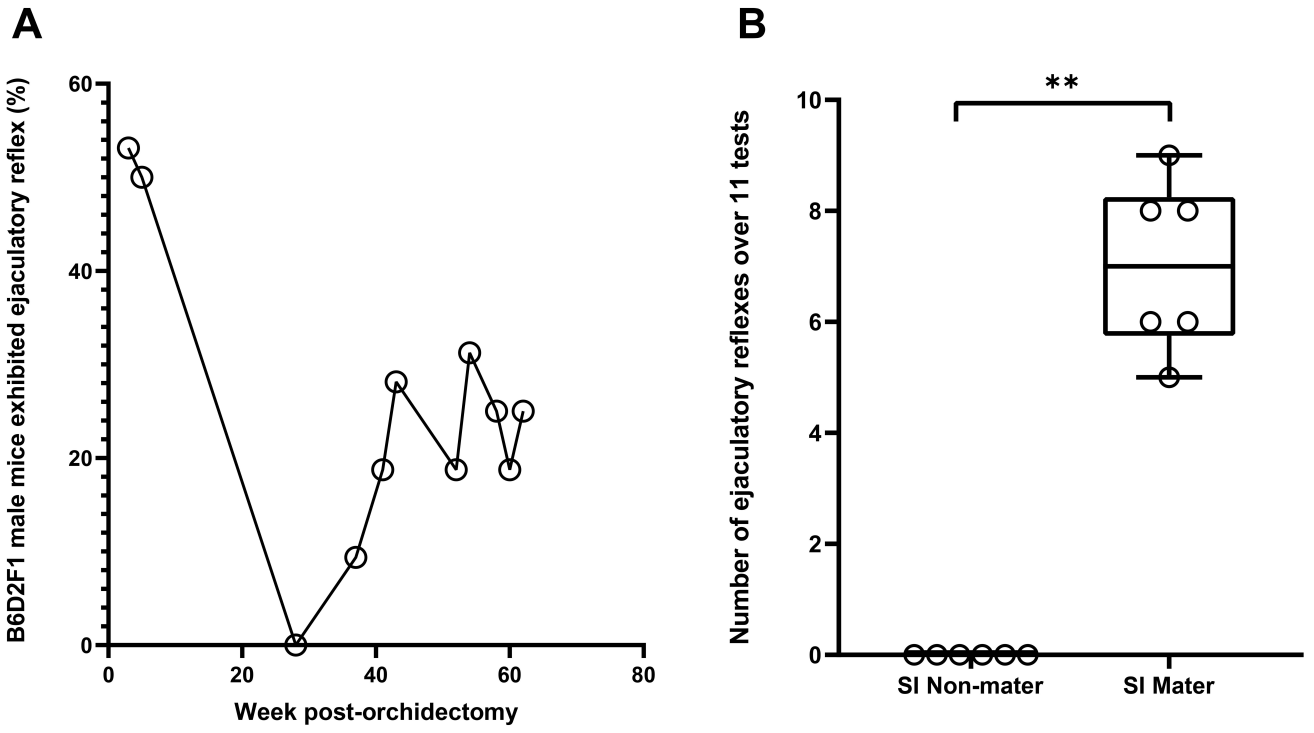
A
B6D2F1 male mice exhibited ejaculatory reflex (%)
60
40
20
0
0
20
40
60
80
Week post-orchidectomy
B
Number of ejaculatory reflexes over 11 tests
10
8
6
4
2
0
**
SI Non-mater
SI Mater

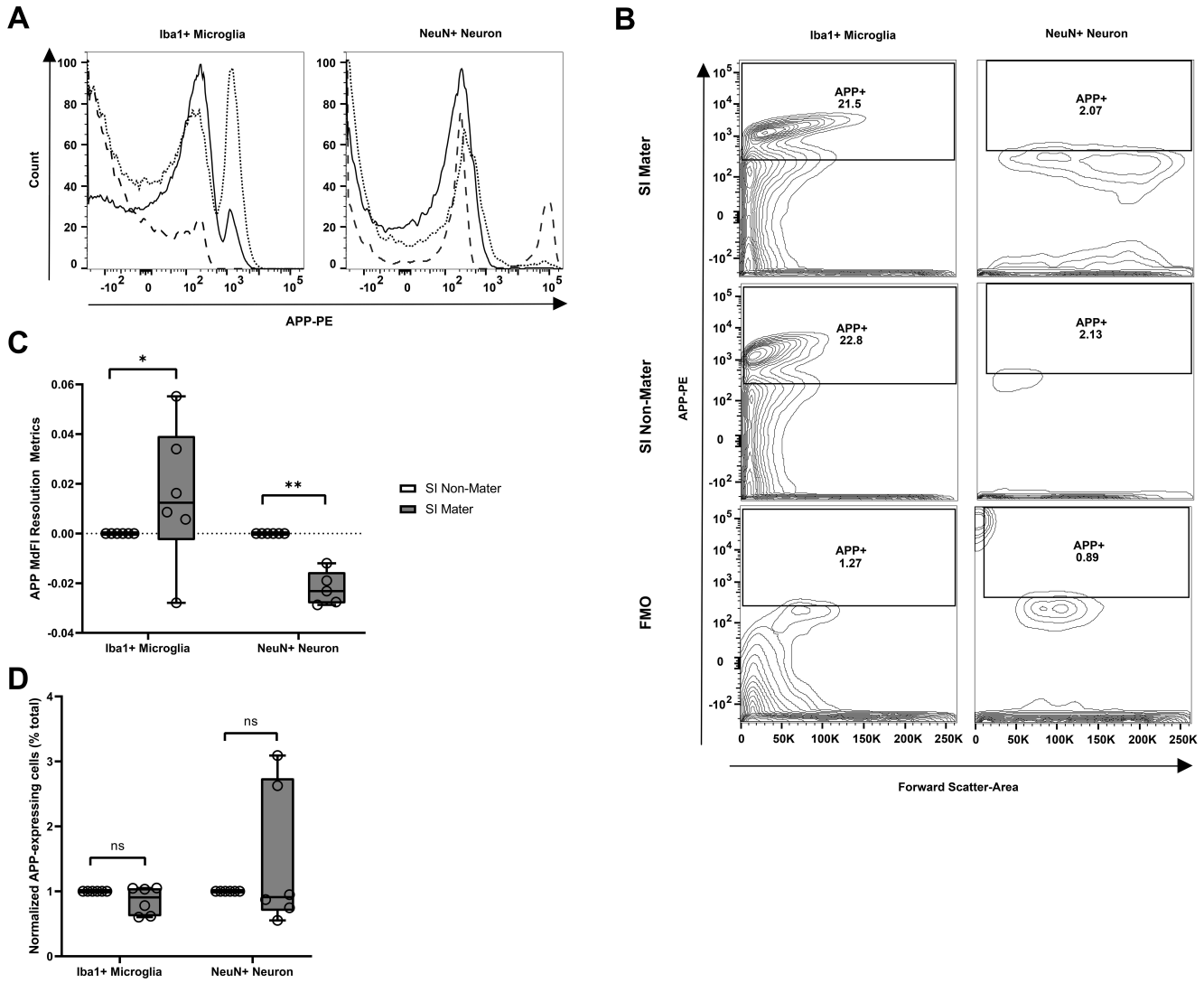
A
Iba1+ Microglia
NeuN+ Neuron
Count
APP-PE
B
Iba1+ Microglia
NeuN+ Neuron
SI Mater
SI Non-Mater
FMO
APP-PE
APP+ 21.5
APP+ 2.07
APP+ 22.8
APP+ 2.13
APP+ 1.27
APP+ 0.89
Forward Scatter-Area
C
APP MdFI Resolution Metrics
SI Non-Mater
SI Mater
Iba1+ Microglia
NeuN+ Neuron
D
Normalized APP-expressing cells (% total)
ns
ns
Iba1+ Microglia
NeuN+ Neuron

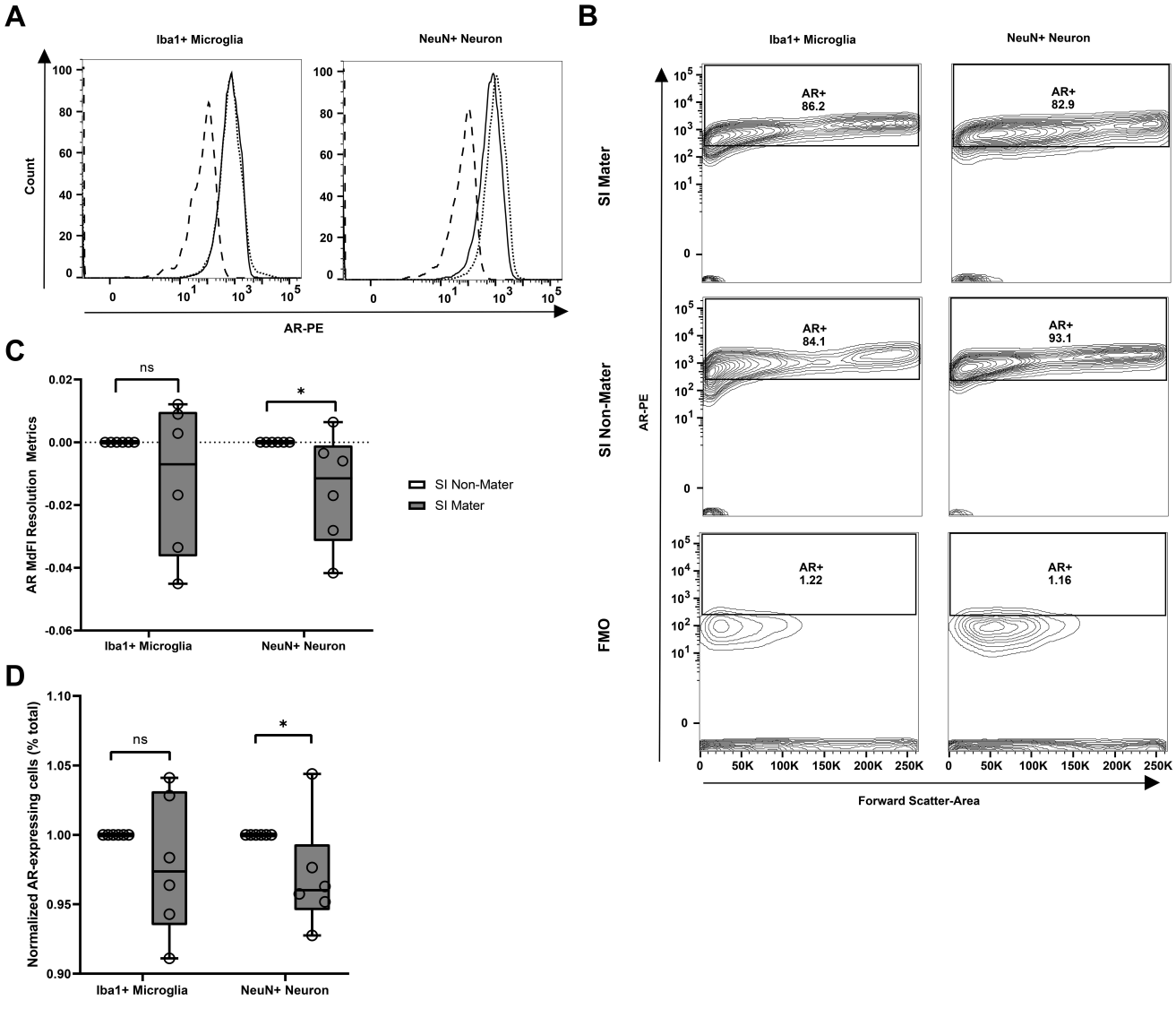
A
Iba1+ Microglia
NeuN+ Neuron
Count
AR-PE
B
Iba1+ Microglia
NeuN+ Neuron
SI Mater
SI Non-Mater
FMO
AR-PE
AR+ 86.2
AR+ 82.9
AR+ 84.1
AR+ 93.1
AR+ 1.22
AR+ 1.16
Forward Scatter-Area
C
ns
*
AR MdFI Resolution Metrics
SI Non-Mater
SI Mater
Iba1+ Microglia
NeuN+ Neuron
D
ns
*
Normalized AR-expressing cells (% total)
Iba1+ Microglia
NeuN+ Neuron

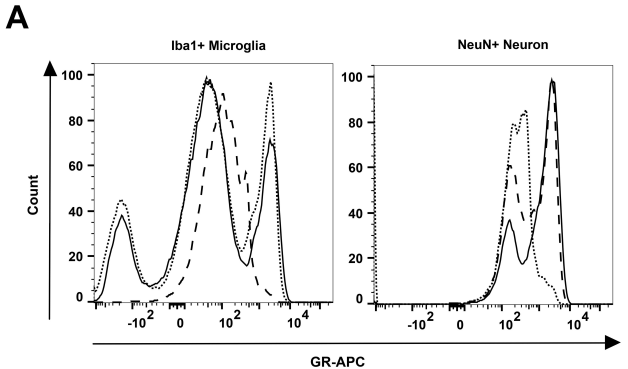
A
Iba1+ Microglia
NeuN+ Neuron
Count
GR-APC

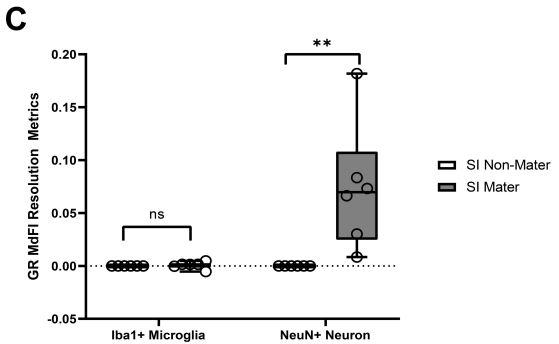
C
GR MdFI Resolution Metrics
ns
**
SI Non-Mater
SI Mater
Iba1+ Microglia
NeuN+ Neuron

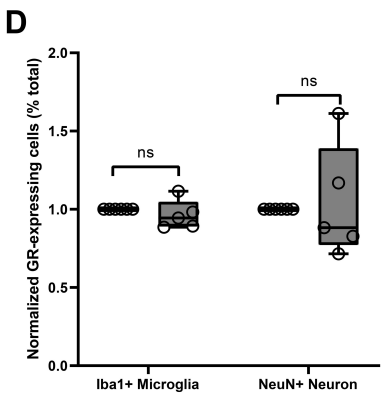
D
Normalized GR-expressing cells (% total)
ns
ns
Iba1+ Microglia
NeuN+ Neuron

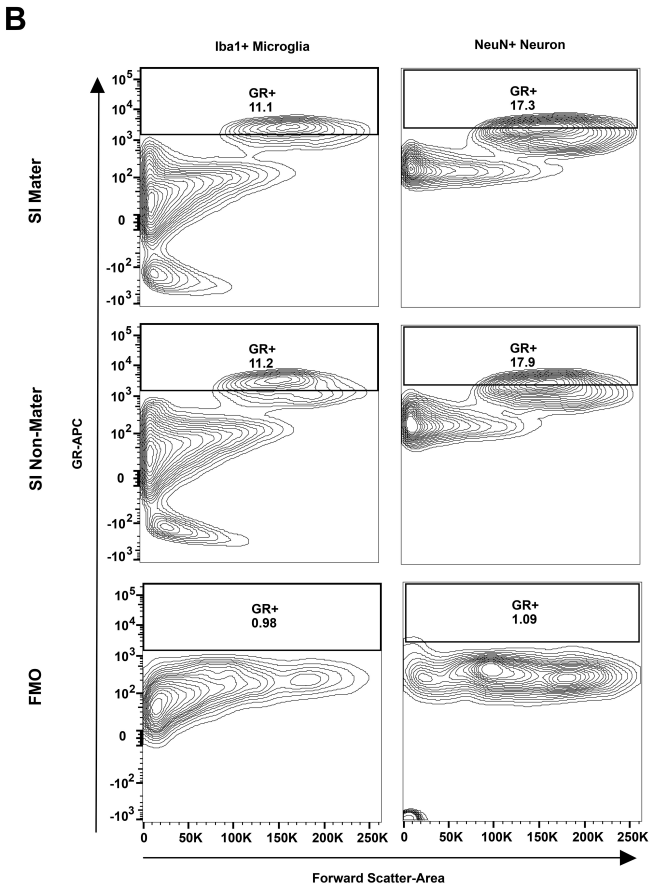
B
Iba1+ Microglia
NeuN+ Neuron
SI Mater
SI Non-Mater
FMO
GR+
11.1
GR+
17.3
GR+
11.2
GR+
17.9
GR+
0.98
GR+
1.09
GR-APC
Forward Scatter-Area

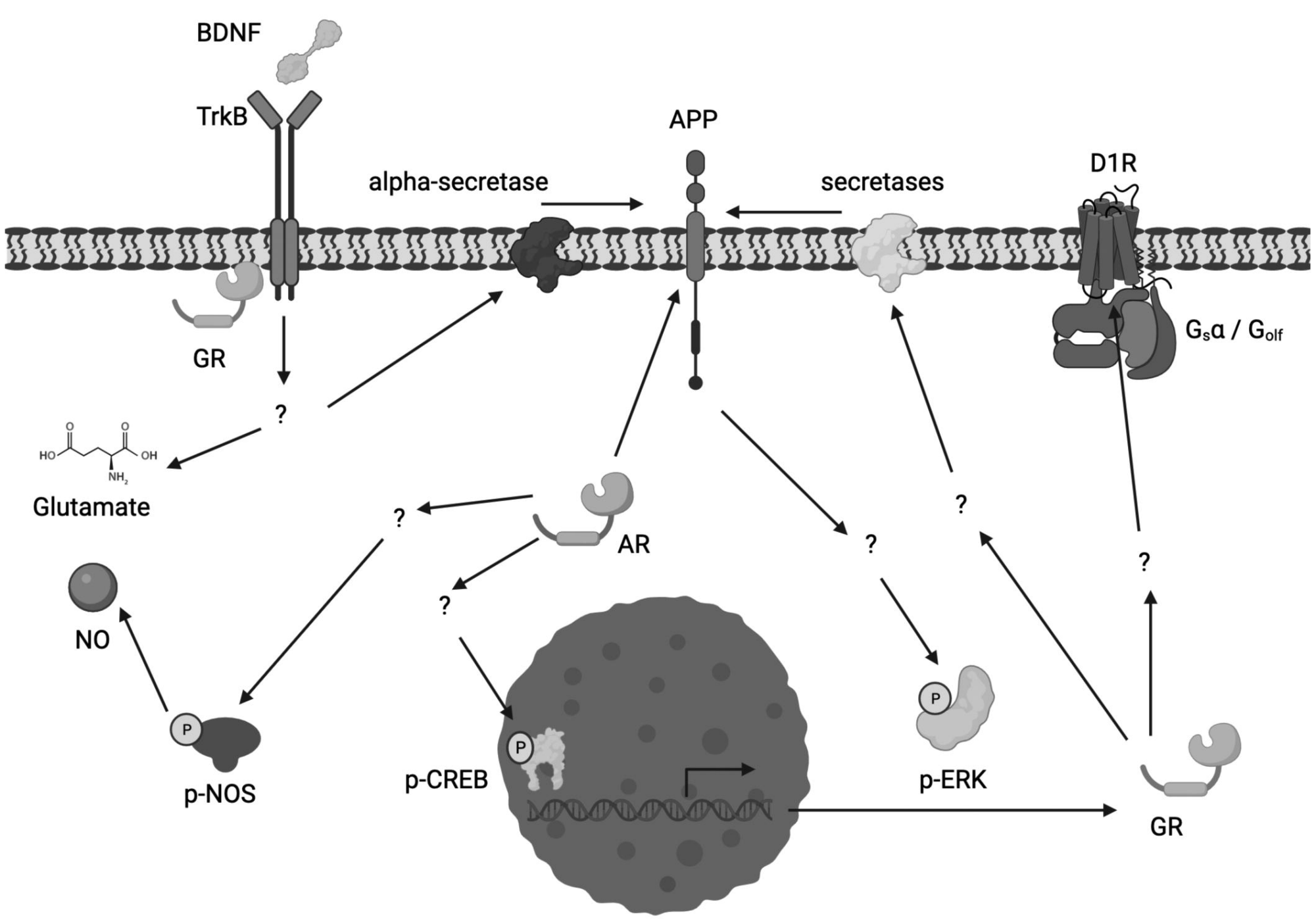
BDNF
TrkB
APP
alpha-secretase
secretases
D1R
GR
$G_s\alpha$ / G_{olf}
?
Glutamate
AR
?
?
?
?
?
NO
P
p-NOS
P
p-CREB
P
p-ERK
GR

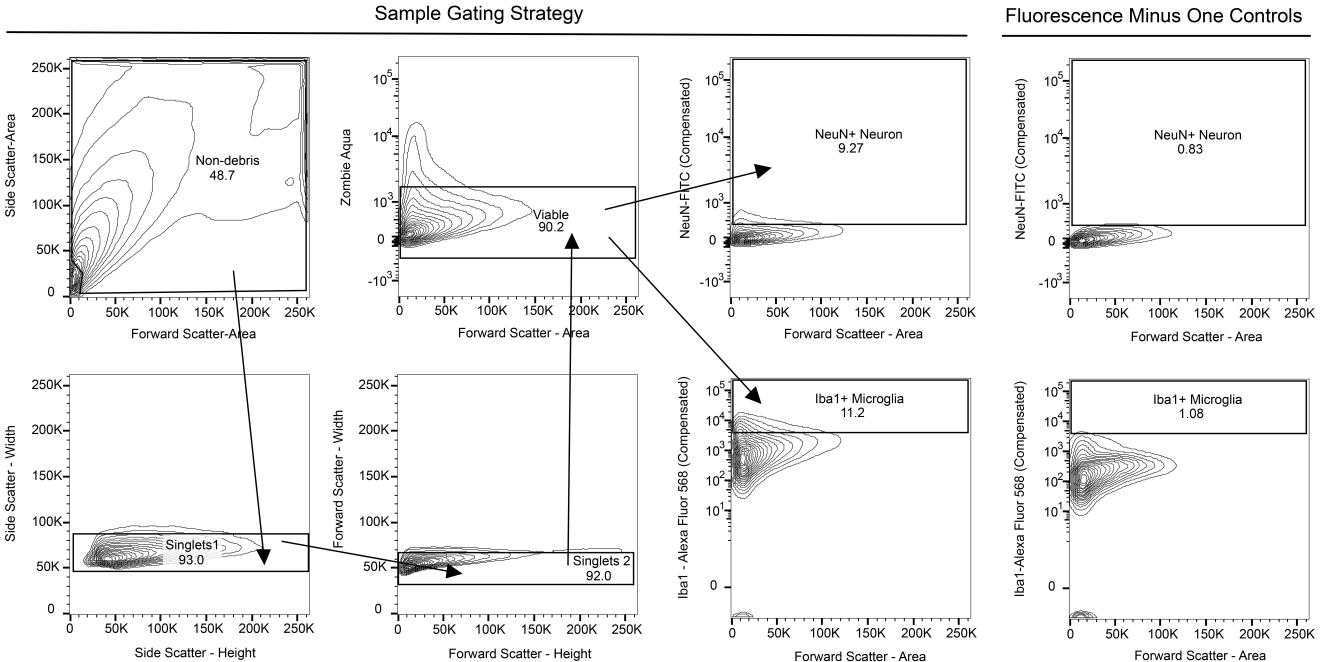
Sample Gating Strategy
Fluorescence Minus One Controls
Side Scatter-Area
Forward Scatter-Area
Non-debris
48.7
Zombie Aqua
Forward Scatter - Area
Viable
90.2
NeuN-FITC (Compensated)
Forward Scatteer - Area
NeuN+ Neuron
9.27
NeuN+ Neuron
0.83
Side Scatter - Width
Side Scatter - Height
Singlets1
93.0
Forward Scatter - Width
Forward Scatter - Height
Singlets 2
92.0
Iba1 - Alexa Fluor 568 (Compensated)
Iba1+ Microglia
11.2
Iba1+ Microglia
1.08

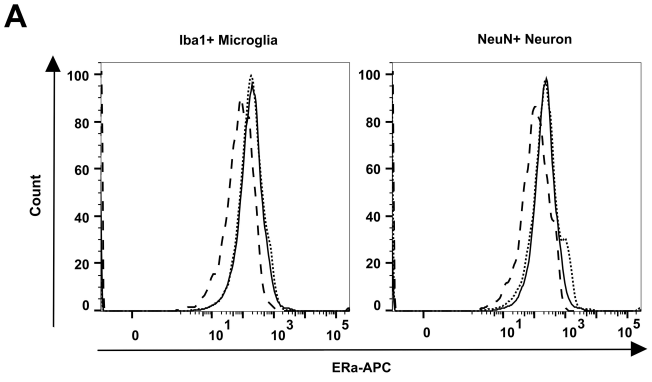
A
Iba1+ Microglia
NeuN+ Neuron
Count
ERa-APC

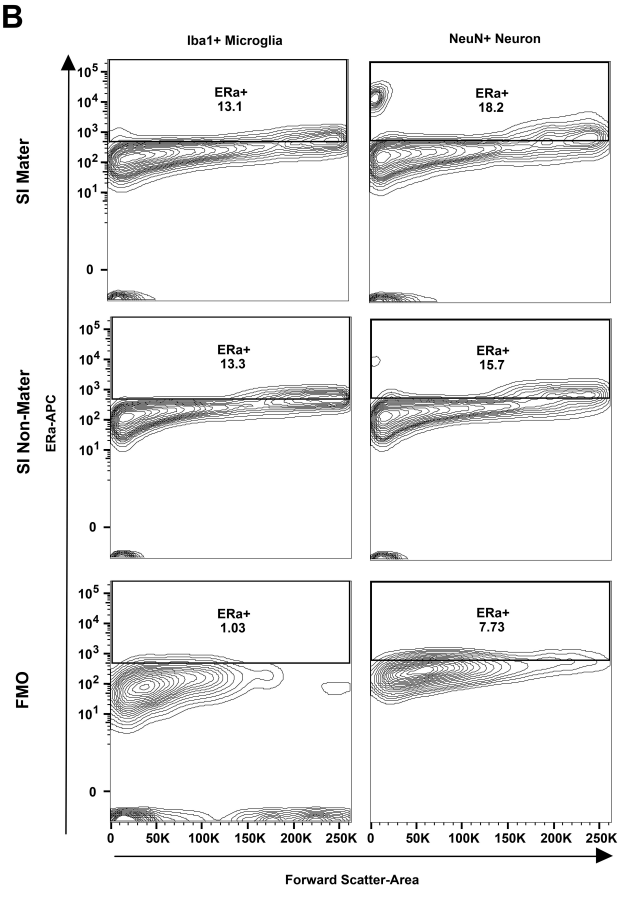
B
Iba1+ Microglia
NeuN+ Neuron
SI Mater
SI Non-Mater
FMO
ERa+
13.1
ERa+
18.2
ERa+
13.3
ERa+
15.7
ERa+
1.03
ERa+
7.73
ERa-APC
Forward Scatter-Area

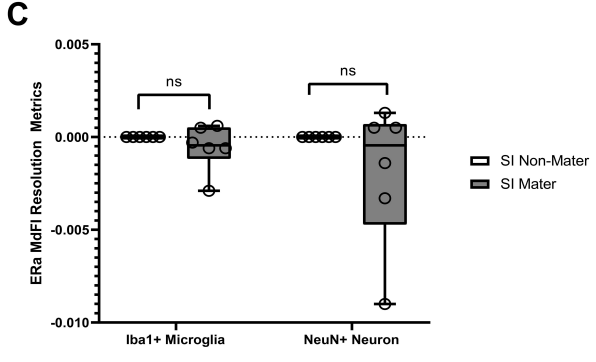
C
ERa MdFI Resolution Metrics
ns
ns
SI Non-Mater
SI Mater
Iba1+ Microglia
NeuN+ Neuron

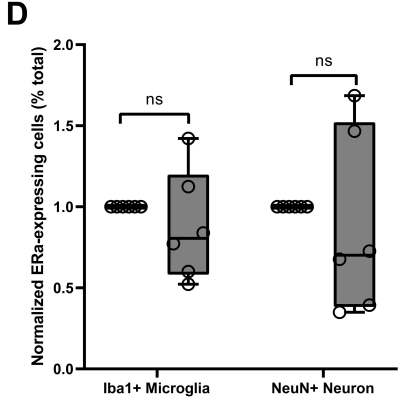
D
Normalized ERa-expressing cells (% total)
ns
ns
Iba1+ Microglia
NeuN+ Neuron